Global exposure of population and land-use to meteorological droughts under different Warming Levels and Shared Socioeconomic Pathways: A Coordinated Regional Climate Downscaling Experiment-based study

Jonathan Spinoni, Paulo Barbosa, Edoardo Bucchignani, John Cassano, Tereza Cavazos, Alessandro Cescatti, Jens Hesselbjerg Christensen, Ole Bøssing Christensen, Erika Coppola, Jason Evans, et al.

Received: 12 February 2021 | Revised: 6 June 2021 | Accepted: 15 July 2021

DOI: 10.1002/joc.7302

RESEARCH ARTICLE

International Journal of Climatology RMetS

Global exposure of population and land-use to meteorological droughts under different Warming Levels and Shared Socioeconomic Pathways: A Coordinated Regional Climate Downscaling Experiment-based study

Jonathan Spinoni[1] | Paulo Barbosa[1] | Edoardo Bucchignani[2,29] | John Cassano[3] | Tereza Cavazos[4] | Alessandro Cescatti[1] | Jens Hesselbjerg Christensen[5,6,28] | Ole Bøssing Christensen[6] | Erika Coppola[7] | Jason Evans[8] | Giovanni Forzieri[1] | Beate Geyer[9] | Filippo Giorgi[7] | Daniela Jacob[11] | Jack Katzfey[12] | Torben Koenigk[13] | René Laprise[14] | Christopher John Lennard[15] | M. Levent Kurnaz[16,17] | Delei Li[18] | Marta Llopart[19] | Niall McCormick[1] | Gustavo Naumann[1] | Grigory Nikulin[13] | Tugba Ozturk[20] | Hans-Jürgen Panitz[21] | Rosmeri Porfirio da Rocha[22] | Silvina Alicia Solman[23,24] | Jozef Syktus[25] | Fredolin Tangang[26] | Claas Teichmann[11] | Robert Vautard[27] | Jürgen Valentin Vogt[1] | Katja Winger[14] | George Zittis[10] | Alessandro Dosio[1]

[1]European Commission, Joint Research Centre (JRC), Ispra, Italy

[2]Centro Euro-Mediterraneo sui Cambiamenti Climatici (CMCC Foundation—REMHI Division), Caserta, Italy

[3]Cooperative Institute for Research in Environmental Sciences (CIRES) and Department of Atmospheric and Oceanic Sciences, Snow and Ice Data Center, University of Colorado, Boulder, Colorado, USA

[4]Centro de Investigación Científica y de Educación Superior de Ensenada (CICESE), Baja California, Mexico

[5]University of Copenhagen, Niels Bohr Institute (NBI), Copenhagen, Denmark

[6]Danish Meteorological Institute, Copenhagen, Denmark

[7]Abdus Salam International Centre for Theoretical Physics (ICTP), Trieste, Italy

[8]Faculty of Science, University of New South Wales, Sydney, Australia

[9]Helmholtz-Zentrum Geesthacht (HZG), Institute of Coastal Research, Hamburg, Germany

[10]The Cyprus Institute (CyI), Climate and Atmosphere Research Center (CARE-C), Nicosia, Cyprus

[11]Climate Service Center Germany (GERICS), Helmholtz-Zentrum Geesthacht, Hamburg, Germany

[12]Commonwealth Scientific and Industrial Research Organisation (CSIRO) Marine and Atmospheric Research, Aspendale, Australia

[13]Swedish Meteorological and Hydrological Institute (SMHI), Rossby Centre, Norrkoping, Sweden

[14]Département des Sciences de la Terre et de l'Atmosphère, Université du Quebec à Montréal (UQAM), Montréal, Canada

[15]University of Cape Town, Climate System Analysis Group (CSAG), Cape Town, South Africa

[16]Department of Physics, Faculty of Arts and Sciences, Bogazici University, Istanbul, Turkey

[17]Center for Climate Change and Policy Studies, Bogazici University, Istanbul, Turkey

[18]Key Laboratory of Ocean Circulation and Waves, Institute of Oceanology, Chinese Academy of Sciences (CAS), Qingdao, China

[19]São Paulo State University and Bauru Meteorological Centre (IPMet/UNESP), Bauru, São Paulo, Brazil

[20]Department of Physics, Faculty of Arts and Sciences, Isik University, Istanbul, Turkey

[21]Institute of Meteorology and Climate Research, Karlsruhe Institute of Technology (KIT), Karlsruhe, Germany

[22]Departamento de Ciências Atmosféricas, Universidade de São Paulo, São Paulo, Brazil

[23]Facultad de Ciencias Exactas y Naturales, Departamento de Ciencias de la Atmósfera y los Océanos (DCAO-FCEN-UBA), Universidad de Buenos Aires, Buenos Aires, Argentina

[24]Universidad de Buenos Aires, Centro de Investigaciones del Mar y la Atmósfera (CIMA/CONICET-UBA), Buenos Aires, Argentina

[25]School of Biological Sciences, The University of Queensland, Brisbane, Australia

[26]Department of Earth Sciences and Environment, The National University of Malaysia (UKM), Bangi, Selangor, Malaysia

[27]National Centre for Scientific Research (CNRS), Institut Pierre-Simon Laplace (IPSL), Laboratoire des Sciences du Climat et de l'Environnement (LSCE), Gif-sur-Yvette, France

[28]NORCE, Norwegian Research Centre AS, Bergen, Norway

[29]Centro Italiano Ricerche Aerospaziali (CIRA), Capua, Italy

Correspondence
Jonathan Spinoni, European Commission—Joint Research Centre, Via enrico Fermi 2749, I-21027, Ispra (VA), Italy.
Email: jonathan.spinoni@ec.europa.eu

Abstract

Global warming is likely to cause a progressive drought increase in some regions, but how population and natural resources will be affected is still underexplored. This study focuses on global population and land-use (forests, croplands, pastures) exposure to meteorological drought hazard in the 21st century, expressed as frequency and severity of drought events. As input, we use a large ensemble of climate simulations from the Coordinated Regional Climate Downscaling Experiment, population projections from the NASA-SEDAC dataset, and land-use projections from the Land-Use Harmonization 2 project for 1981–2100. The exposure to drought hazard is presented for five SSPs (SSP1-SSP5) at four Global Warming Levels (GWLs, from 1.5 to 4°C). Results show that considering only Standardized Precipitation Index (SPI; based on precipitation), the combination SSP3-GWL4 projects the largest fraction of the global population (14%) to experience an increase in drought frequency and severity (vs. 1981–2010), with this value increasing to 60% if temperature is considered (indirectly included in the Standardized Precipitation-Evapotranspiration Index, SPEI). With SPEI, considering the highest GWL for each SSP, 8 (for SSP2, SSP4, and SSP5) and 11 (SSP3) billion people, that is, more than 90%, will be affected by at least one unprecedented drought. For SSP5 (fossil-fuelled development) at GWL 4°C, approximately $2{\cdot}10^6$ km^2 of forests and croplands (respectively, 6 and 11%) and $1.5{\cdot}10^6$ km^2 of pastures (19%) will be exposed to increased drought frequency and severity according to SPI, but for SPEI, this extent will rise to $17{\cdot}10^6$ km^2 of forests (49%), $6{\cdot}10^6$ km^2 of pastures (78%), and $12{\cdot}10^6$ km^2 of croplands (67%), with mid-latitudes being the most affected areas. The projected likely increase of drought frequency and severity significantly increases population and land-use exposure to drought, even at low GWLs, thus extensive mitigation and adaptation efforts are needed to avoid the most severe impacts of climate change.

KEYWORDS

climate projections, CORDEX, drought, global warming levels, land-use, population, socioeconomic scenarios

1 | INTRODUCTION

From a meteorological point of view, drought events are usually associated with prolonged deficits of precipitation, high temperatures, dry winds, and low humidity (Mishra and Singh, 2010). Compared to other natural hazards as floods or windstorms, droughts are slowly developing and more complex events (Wilhite, 2000) and, because it is not possible to define them in a unique way (Lloyd-Hughes, 2014), multivariate perspective (Hao and Singh, 2015), advanced modelling (Mishra and Singh, 2011), and specific indicators (Heim Jr, 2002; Zargar *et al*., 2011) are required to characterize and study them. Mega-droughts such as the California drought in 2012–2014 (Griffin and Anchukaitis, 2014), the Millennium Drought in Australia (Van Dijk *et al*., 2013), the multi-year drought in South Africa in 2015–2017 (Otto *et al*., 2018), the decennial drought in central Chile (Garreaud *et al*., 2020), and other recent drought-related disasters (Below *et al*., 2007; Cook *et al*., 2016) also show that quantifying drought impacts can be challenging (Blauhut *et al*., 2015).

Despite such difficulties, in the last decades, the scientific community made significant efforts to investigate drought risk at global (Carrao *et al*., 2016; Carrão *et al*., 2018; Meza *et al*., 2020) and country scales (Wilhite *et al*., 2014; Kim *et al*., 2015); such risk is projected to progressively increase in many regions in the 21st century (Cook *et al*., 2015; Cook *et al*., 2020) due to global warming (IPCC, 2014). An increasing probability of severe or extreme droughts requires adequate mitigation and adaptation policies to prevent and limit their impacts and recover from their consequences (Wilhite *et al*., 2007; Taylor *et al*., 2013; Schwalm *et al*., 2017), and to optimize the costs of interventions (Logar and van den Bergh, 2013), especially in regions of acknowledged severe risk (e.g., the Mediterranean region Iglesias *et al*., 2007; Vogt and Somma, 2000).

According to the Intergovernmental Panel on Climate Change (IPCC; Field *et al*., 2012), risk can be characterized by three components: hazard, exposure, and vulnerability. Drought hazard is by far the most studied component, and many works have investigated past and future drought trends. At global scale, especially in recent decades, observed drought frequency and severity showed small increase (Seneviratne, 2012; Sheffield *et al*., 2012; Spinoni *et al*., 2019), which is more pronounced if temperature is taken into account in the drought index formulation (Trenberth *et al*., 2014) instead of considering only precipitation (Spinoni *et al*., 2014). A few hotspots emerge, including southern South America, the Mediterranean region, and southern Africa (Greve *et al*., 2014).

On the other hand, drought hazard projections show a high degree of complexity, also because of inherent uncertainties in climate models, especially for precipitation and over some regions of the world (Ficklin *et al*., 2016; Dosio *et al*., 2019). This could lead to uncertain drought projections (Dai and Zhao, 2017; Zhao and Dai, 2017), an issue affecting different generations of models (Burke and Brown, 2008; Orlowsky and Seneviratne, 2013). Being aware that such uncertainties cannot be totally neglected, some studies reported that future drought hazard is likely to increase more steeply in the future than in the recent past, especially under the most severe emission scenarios (Cook *et al*., 2014; Zhao and Dai, 2015). The role of temperature in future droughts is more pivotal than for the past (Ahmadalipour *et al*., 2017), especially over regions where future drought tendencies are spatially inhomogeneous, for example, Europe (Spinoni *et al*., 2018) and the United States (Jeong *et al*., 2014).

Global projections of meteorological droughts are commonly based on Global Climate Models (GCMs), whose low spatial resolution limits their ability to simulate local processes (Cook *et al*., 2014) in regions of complex topography and heterogeneous land-use (Xu *et al*., 2019a). Recently, Spinoni *et al*. (2020) published the first study on drought projections at global scale based on Regional Climate Models (RCMs) from the Coordinated Regional-climate Downscaling Experiment (CORDEX; Giorgi and Gutowski Jr, 2015). This study was the first to apply CORDEX data at global scale, although RCMs have already been used for drought studies at continental (e.g., Europe: Spinoni *et al*., 2018), macro-regional (e.g., Middle-East and North Africa: Driouech *et al*., 2020; West Africa: Diasso and Abiodun, 2017; South Asia: Samantaray *et al*., 2021), and country scales (e.g., South Korea: Nam *et al*., 2015).

At the 21st Conference of the Parties in Paris (COP21; UNFCCC, 2015), signatory countries agreed to keep global warming below 2°C above pre-industrial levels, with the aim of limiting it to 1.5°C (Hare *et al*., 2016). Since then, studies assessing the impact of climate change under specific Global Warming Levels (GWLs) are becoming increasingly common (IPCC, 2018). In this study, we compute drought projections at specific GWLs (from 1.5 to 4°C). Compared to previous works, the combined use of GCMs and RCMs at global scale (for a total of around 150 simulations), the spatial resolution (0.44°), and the critical investigation of the key role of temperature make this study a significant step forward.

Compared to drought hazard, the number of scientific publications investigating exposure to drought is smaller, but local studies focusing on the exposure of population or single land-use categories are not rare; examples

include impacts on mental (O'Brien *et al*., 2014) and physical health (Ebi and Bowen, 2016), poverty (Winsemius *et al*., 2015), children undernutrition (Hirvonen *et al*., 2020), social issues (Wilhite and Buchanan-Smith, 2005; Below *et al*., 2007), forest ecosystems (Grossiord *et al*., 2014), pastures (Rolo and Moreno, 2019), or croplands (Peduzzi *et al*., 2009). Such studies often focuses on developing countries as sub-Saharan regions (Gray and Mueller, 2012; Kamali *et al*., 2018), but there are also a few related to other countries as, for example, Australia (Kiem *et al*., 2016), China (Zhang *et al*., 2011), and South Korea (Kim *et al*., 2015). The effects of recurrent severe droughts on population are known to be highly impacting in least developed countries (Miyan, 2015; Marengo *et al*., 2017), affecting especially early child health (Kumar *et al*., 2016), and possibly forcing poverty and migration (Sheffield and Wood, 2011; Ahmadalipour *et al*., 2019), and such effects could increase in a warming world (Liu *et al*., 2018; Gu *et al*., 2020).

Forests are known to be vulnerable to climate change and drought (Choat *et al*., 2012; Hlásny *et al*., 2014) and in general to natural hazards (Seidl *et al*., 2017; McDowell *et al*., 2020) that could lead to increased tree mortality due to a decreased ability to survive insect outbreaks (Kurz *et al*., 2008) or forest fires (Boer *et al*., 2020) in case of, for example, combination with extreme heat-waves (Rennenberg *et al*., 2006) or devastating events such as the California droughts in 2012–2015 (Asner *et al*., 2016). Also pastures are known to be affected by climate change (Tubiello *et al*., 2007; Cullen *et al*., 2009; Perera *et al*., 2019), and in particular droughts (Ding *et al*., 2011), which can even be a contributory cause of land abandonment (Doblas-Miranda *et al*., 2017), and whose effects are likely to increase in coming decades (Soussana *et al*., 2010). Similar impacts are expected in agricultural production (Gornall *et al*., 2010; Schwalm *et al*., 2012; Swain and Hayhoe, 2015; Cook *et al*., 2018), which could suffer from serious yield reductions and decreased crop productions (Lesk *et al*., 2016; Zampieri *et al*., 2017; Toreti *et al*., 2019) during and following severe events like the droughts in the 2010's in Russia (Wegren, 2011), China (Zhang *et al*., 2012), and California (Howitt *et al*., 2014; Medellín-Azuara *et al*., 2016).

This study aims at improving our understanding of future exposure to droughts of population and natural ecosystems at different GWLs under several shared socio-economic pathways (SSPs; O'Neill *et al*., 2014, 2017). The regions projected to face more frequent and severe droughts, sometimes aggravated by anthropogenic factors (Seager *et al*., 2015; Williams *et al*., 2015), are likely to see a consequential increase in drought risk (Cook *et al*., 2015), sometimes leading to irreversible land degradation and desertification (Reed and Stringer, 2016). Therefore, global drought projections could help implementing mitigation (Taylor *et al*., 2013) and adaptation policies (Logar and van den Bergh, 2013).

This article is structured as follows: Section 2 (Data and Methods) describes input climate and land-use data, drought indicators and derived parameters, and details on RCPs and SSPs; Section 3 (Results and Discussion) presents drought hazard and exposure projections at continental and macro-regional scales, with special focus on the role of temperature for droughts and on the SSP5 scenario (fossil-fuelled development; Kriegler *et al*., 2017); Section 4 (Conclusions) sums up the main findings and anticipates the next steps.

2 | DATA AND METHODS

2.1 | Climate data

To compute drought indicators and derived parameters we started from meteorological variables from the CORDEX datasets: monthly precipitation (P), minimum (T_N), and maximum temperature (T_X) for the period 1981–2100. For each of the 14 CORDEX domains (see: www.cordex.org), we obtained all possible combinations of GCMs and RCMs that provided both precipitation and temperature data for the moderate Representative Concentration Pathway RCP4.5 (Thomson *et al*., 2011) and extreme RCP8.5 (Riahi *et al*., 2011). We excluded the RCP2.6 and the RCP6.0 (van Vuuren *et al*., 2011a; 2011b), because of their unavailability for most CORDEX domains.

To ensure spatial homogeneity, we selected simulations at comparable spatial resolution (approximately 0.44°), thus excluding higher resolution subsets over single domains as the EURO-CORDEX (0.11°; Jacob *et al*., 2014) and the new simulations from CORDEX-CORE at 0.22° (Gutowski *et al*., 2016; Giorgi *et al*., 2017). The full list of simulations includes 23 CMIP5 GCMs combined with 33 RCMs (Table 1), which leads to a heterogeneous number of GCM-RCM combinations at global scale, from a minimum of 16 over Antarctica to a maximum of 145 over the Middle-East, counting both RCPs (Figure S1). Compared to Spinoni *et al*. (2020), the number of simulations increased by around 40% and we used only the simulations with no reported outliers and unrealistic values, and with complete metadata. Despite the unprecedented number of simulations, the interpolation of single models over a common 0.44° grid did not produce biases at borders between CORDEX domains, as no border shows precipitation and mean temperature discontinuities—averaged over 1981–2010—respectively,

TABLE 1 List of simulations used in this study

GCM	RCM				
CCCma-CanESM2	CCCma-CanRCM4	IITM-RegCM4-4	SMHI-RCA4	UQAM-CRCM5	
CMCC-CM	CMCC-CCLM4-8-19				
CNRM-CERFACS-CNRM-CM5	HMS-ALADIN52	CLMcom-CCLM4-8-17	CLMcom-CCLM-5-0-2	CLMcom-CCLM5-0-6	CNRM-ALADIN52
	CNRM-ALADIN53	CSIRO-CCAM	IITM-RegCM4-4	RMIB-Ugent-ALARO-0	SMHI-RCA4
CSIRO-BOM-ACCESS1-0	CSIRO-CCAM				
CSIRO-BOM-ACCESS3-0	CSIRO-CCAM				
CSIRO-QCCCE-MK3-6-0	CSIRO-CCAM	IITM-RegCM4-4	SMHI-RCA4		
ICHEC-EC-EARTH	CLMcom-CCLM4-8-17				
	CLMcom-CCLM4-8-17-CLM3-5	CLMcom-CCLM-5-0-2	CLMcom-CCLM5-0-6	DMI-HIRHAM5	KNMI-RACMO21P
	KNMI-RACMO22E	KNMI-RACMO22T	MPI-CSC-REMO2009	SMHI-RCA4	SMHI-RCA4-SN
	UniLund-RCA4-GUESS				
IPSL-IPSL-CM5A-LR	IITM-RegCM4-4	GERICS-REMO2009			
IPSL-IPSL-CM5A-MR	IPSL-INERIS-WRF331F	LMD-LMDZ4NEMOMED8	SMHI-RCA4		
MIROC-MIROC5	CLMcom-CCLM5-0-6	CSIRO-CCAM	GERICS-REMO2009	SMHI-RCA4	
MOHC-HadGEM2-ES	BOUN-RegCM4-3.5	CLMcom-CCLM4-8-17	CLMcom-CCLM-5-0-2	CLMcom-CCLM5-0-6	CSIRO-CCAM
	GERICS-REMO2009	ICTP-RegCM4-3	KNMI-RACMO21P	KNMI-RACMO22E	KNMI-RACMO22T
	NCAR-AZ-WRF	NCAR-RegCM4	SMHI-RCA4		
MOHC-HadGEM2-AO	MOHC-HadGEM3-RA				
MPI-M-MPI-ESM-LR	CLMcom-CCLM4-8-17	CLMcom-CCLM4-8-17-CLM3-5	CLMcom-CCLM-5-0-2	CLMcom-CCLM5-0-6	CSIRO-CCAM
	GUF-CCLM-4-8-18	ICTP-RegCM4-3	MGO-RRCM	MPI-CSC-REMO2009	NCAR-AZ-WRF
	NCAR-RegCM4	SMHI-RCA4	SMHI-RCA-SN	UQAM-CRCM5	
MPI-M-MPI-ESM-MR	BOUN-RegCM4-3.5	ICTP-RegCM4-3	IITM-RegCM4-4	SMHI-RCA-SN	UQAM-CRCM5
NCAR-CCSM4	CSIRO-CCAM				
NCAR-CESM1	CYI-WRF351				
NCC-NorESM1-M	CSIRO-CCAM	DMI-HIRHAM5	SMHI-RCA4		
NOAA-GFDL-GFDL-CM3	CSIRO-CCAM				
NOAA-GFDL-GFDL-ESM2G	GERICS-REMO2009				
NOAA-GFDL-GFDL-ESM2M	CSIRO-CCAM	IITM-RegCM4-4	NCAR-AZ-WRF	NCAR-RegCM4	SMHI-RCA4
UQAM-GEMatm-can	UQAM-CRCM5				
UQAM-GEMatm-MPI	UQAM-CRCM5				
UQAM-GEMatm-MPI-ESMsea	UQAM-CRCM5				

larger than 5% and 1°C, excluding the Urals for temperature. Similar multi-domain approaches have already been used for different regions, for example, by Zittis *et al*. (2019) and Legasa *et al*. (2020).

Observed precipitation and temperature data for validation include the latest version of the Deutscher Wetterdienst's Global Precipitation Climatology Centre (GPCC version 8; Schneider *et al*., 2018) and the University of East Anglia's Climate Research Unit (CRU TS version 4.04; Harris *et al*., 2020) datasets.

Here, we focus on the GWLs, following the methodology of Dosio and Fischer (2018) (also used in previous studies, for example, Vautard *et al*. (2014), Kjellström *et al*., 2018). First, we define 1981–2010 as reference period and we derive the global (considering both land and oceans) temperature increase compared to the pre-industrial values (1881–1910; but other intervals can be selected, see Hawkins *et al*., 2017) of the selected reference period, which is 0.96°C according to NASA Goddard's Global Surface Temperature Analysis dataset (GISTEMPv4; Hansen *et al*., 2010). Second, for each GCM run (and either RCP), we look for the first year (obtained from running mean values) corresponding to an additional warming by 0.54°C (1.04, 2.04, and 3.04°C) compared to the reference period. Thus, the 30-year period centred on that year corresponds to a GWL of 1.5°C (2, 3, and 4°C) for that run. With this approach, where the GWLs are defined by using GCMs and therefore applied to RCMs (see Dosio *et al*., 2018), the climate and drought quantities are calculated for 30-year periods corresponding to GWLs: for most GCM runs, RCP8.5 allows reaching all GWLs considered in this study, while RCP4.5 allows reaching 1.5 and 2°C only.

2.2 | Drought hazard indicators and derived parameters

All calculations from input variables to drought indicators and parameters are firstly performed at every grid point for each simulation (and RCPs) at each grid point, and then re-gridded over a common 0.44° grid. The output drought-related quantity eventually represents the ensemble median of the corresponding variable.

Thus, for a given model, scenario, and grid point, we use precipitation data to obtain the Standardized Precipitation Index (SPI, McKee *et al*., 1993) and precipitation and temperature data to obtain the Standardized Precipitation-Evapotranspiration Index (SPEI; Vicente-Serrano *et al*., 2010; Beguería *et al*., 2014). The two indicators, both computed at 12-month scale (SPI-12 and SPEI-12) scale to avoid excessive variability typical of shorter accumulation periods (Cook *et al*., 2014), are computed using the entire period 1981–2100 as baseline. Separating SPI-12 and SPEI-12 allows us to investigate the role of temperature in meteorological drought projections, only (indirectly) present in SPEI, which is based on the difference between precipitation and potential evapo-transpiration (PET). PET is calculated using the Hargreaves-Samani equation (Hargreaves and Samani, 1985), based on minimum and maximum temperature, and latitude. The methodology to obtain PET and its use for drought has been widely discussed in the scientific literature; see Donohue *et al*. (2010), Trenberth *et al*. (2014), and Spinoni *et al*. (2017).

Once we obtain monthly time series of SPI-12 and SPEI-12 for 1981–2100, we adapt the theory of runs (Yevjevich, 1967) to define the occurrence of a meteorological drought event: it starts when SPI-12 (same holds for SPEI-12) goes below −1 for at least two consecutive months and ends when the indicator goes above 0 for at least two consecutive months. The number of drought events in a period is called drought frequency (DF). Over each period, we also calculate the average severity of drought events (DS), computed as the sum over the negative indicator values (in absolute values) during the event, and the unprecedented drought events (PK), that is, the number of events in a future period more severe than the most severe in 1981–2010.

Thus, for each GCM-RCM run (and either RCP), we compute DF and DS for 1981–2010 and DF, DS, and PK for four GWLs, namely, 1.5, 2, 3, and 4°C. Subsequently, we calculate the ensemble median of these quantities from all the GCMs-RCMs and RCPs combinations available for that grid point (following Feyen *et al*., 2020), assuming that the different land-use parameterizations included in the two RCPs have very limited impact on climate-based projections. This approach focuses on GWLs irrespectively of how and when they have been reached, assuming that the spatial distribution of climate variables (and their variability) is the same at the same GWL, independent of the scenario. Such an approach has been frequently applied in recent drought-related studies (Samaniego *et al*., 2017; Marx *et al*., 2018; Samaniego *et al*., 2018) and, though the mentioned assumptions are a source of uncertainties, they are not generally affecting the main results when dealing with drought.

Following Spinoni *et al*. (2020), we define that the change in an index is significant in sign if two-thirds of simulations agree on the sign of change, significant in magnitude if the ensemble median change is larger than the inter-model variability over 1981–2010, robust if the change is both significant in sign and magnitude, uncertain if the change is not significant in sign nor in magnitude. Results are shown at different aggregation scales: global, continental, and macro-regional, and macro-regions are defined according to Iturbide *et al*. (2020) and are shown in Figure S2.

2.3 | Population and land-use data

To investigate future global population exposure to droughts, we use global population projections from the NASA-SEDAC datasets (Jones and O'Neill, 2016). We apply the newest available version (v1.01) at 0.125° resolution for the period 2000–2100, qualitatively and quantitatively consistent with the SSPs (Jones and O'Neill, 2020). Such projections divide between urban and rural population, but we use total population and we assume that the base year (2000) represents 1981–2010. We use data for five SSPs: green growth (SSP1; van Vuuren *et al*., 2017), middle of the road (SSP2; Fricko *et al*., 2017), regional rivalry (SSP3; Fujimori *et al*., 2017), deepening inequality (SSP4; Calvin *et al*., 2017), and fossil-fuelled development (SSP5; Kriegler *et al*., 2017). Figure S3 shows the macro-regional population changes in the 21st century according to the five SSPs.

Besides population, we investigate the future exposure to drought of forests, pastures, and croplands. As land-use data, we use the harmonized set of scenarios by the Land-Use Harmonization project 2 (LUH2), based on the estimation of annual fractional land-use patterns and transitions, and agricultural management information, from 850 to 2100 at 0.25° resolution (Hurtt *et al*., 2018). To ensure consistency with population projections, we use land-use data following the same SSPs.

LUH2 data can be grouped into five main classes: primary (never impacted by human activities) and secondary (recovering from human disturbance) vegetation, urban, croplands, and pastures. In this study, we focus on croplands (including all five crop types: C_3 annual and perennial, C_4 annual and perennial, and C_3 nitrogen fixing), pastures (considering only managed pastures and excluding rangelands), and forests (derived from the forested fractions of both primary and secondary vegetation). LUH2 is primarily a land-use product and its focal point is the human use of land, so the distinction of vegetation into forested and non-forested areas can be seen as first-order land cover classification not free from uncertainties (see https://luh.umd.edu/faq.shtml for details). In Supporting Information, we show the land-use changes from 1981–2010 to 2100 (Figure S4).

2.4 | Exposure to drought—combining climate and socio-economic scenarios

In order to assess the exposure to droughts under different combinations of climatic and socio-economic conditions, it is necessary to determine the compatibility between GWLs and SSPs (Rogelj *et al*., 2012; IPCC, 2014; Van Vuuren and Carter, 2014; O'Neill *et al*., 2016). Table S1 summarizes the viable combinations: SSP1 is compatible with GWL of 1.5°C, SSP2 up to 2°C, SSP4 up to 3°C, and both SSP3 and SSP5 up to a 4°C warming.

Each of the SSPs is provided with parent global temperature projections for 21st century (Riahi *et al*., 2017; see also: https://tntcat.iiasa.ac.at/SspDb/). To each SSP, we assign the year corresponding to the GWL effectively reached under its development trajectory. Therefore, for each SSP, we select population values corresponding to the year representing the GWL (which therefore represents the average of a 10-year window, see Table S2) while for land-use classes we use the average values of a 10-year window centred over the year representing the GWL.

Here, we estimate the projected population and land-use exposure to an increase in DF and DS of drought events, but we highlight that estimates of exposure do not incorporate vulnerability components. Moreover, we refer to total population, therefore an increase in the hazard in the grid cell corresponding to a mega-city result in a much larger increase in percentage of exposed population compared to an increase in hazard in sparsely inhabited areas. Dealing with land-use, we refer to fractions of the grid covered without accounting for different productivity, which could play a relevant role—in particular for forests (Keeling and Phillips, 2007) and croplands (Knox *et al*., 2012)—but is partially reflected in the cover fractions. However, we focus on fractions, and consequently total extent exposed, as global high-resolution productivity projections of forests, croplands, and pastures under multiple SSPs are not yet available.

3 | RESULTS AND DISCUSSION

3.1 | Drought hazard projections

Before investigating future drought hazard and in order to exclude systematic biases, we compared DF and DS over 1981–2010 derived from observed data (GPCC and CRU) with the results from the CORDEX ensemble (-Figure S5). CORDEX runs have been thoroughly evaluated over several domains, not only with respect to mean climatology but also extreme events (Akinsanola and Zhou, 2019; Supari *et al*., 2020; Tamoffo *et al*., 2020; Tangang *et al*., 2020) and physical processes (Careto *et al*., 2018; Pattnayak *et al*., 2018; Ashfaq *et al*., 2020). Therefore, we present a basic evaluation of the main drought variables. The overall agreement between simulations and observations is satisfactory and no systematic biases are found, apart from a slight underestimation of DS by the simulations at tropical latitudes. Areas where biases in DS and DF are larger than 10% are mainly

located over northwestern Amazonia and the Democratic Republic of the Congo, where simulations overestimate DF and underestimate DS. Notably, these regions are known for the sparse network of rainfall gauge stations and, consequently, prone to observational uncertainty (Schneider *et al*., 2011; Harris *et al*., 2020).

The first aim of this study is to assess where and to what extent meteorological droughts are likely to become more frequent and severe in a progressively warmer world. For DF, results are shown in Figure 1: if SPI is considered, most areas at mid and high latitudes in the Northern Hemisphere show a decrease in DF linked to increasing projected precipitation (Figure S6 and Table S3), especially above 3°C warming. Under such warming, an increase in DF becomes robust over Mexico, southern South America, the Mediterranean region, and southern Africa. On the other hand, if SPEI is considered, most of the land areas of the World—excluding high latitudes in both Hemispheres and southwestern Asia—are projected to experience an increase in DF, which becomes progressively larger with increasing GWL. In particular, the increase is robust for the Western United States already at GWL 1.5°C, while at 4°C warming most of the regions are projected to face a DF increase up to more than two events/decade compared to 1981–2010. Differences in DF between 1.5 and 2°C warming are larger at high latitudes for SPI (decrease), and at tropical and mid-latitudes for SPEI (increase). Results over ice caps (and hot or cold deserts) are difficult to interpret, because monthly rainfall is usually very low there, so that small variations could be misled for large deviations from normal (Charney *et al*., 1975; Pomeroy *et al*., 2007).

Not surprisingly, the projections for DS show spatial and temporal patterns like those of DF (Figure S7), but in this case the decreasing tendencies based on SPI are already robust at low GWLs over cold regions in both Hemispheres. Such regions also exhibit the largest inter-model spread, although DS overall shows smaller inter-model variability than DF (both evaluated with the standard deviation of the ensemble), which, in turn, shows smaller values for SPI than for SPEI (Figure S8).

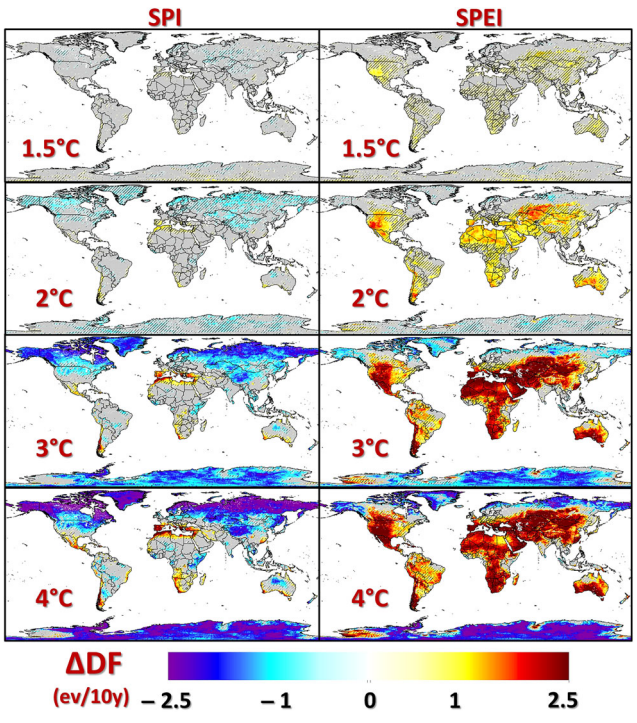

FIGURE 1 Change in drought frequency (DF) between 1981 and 2010 and periods corresponding to GWLs according to SPI and SPEI. Areas where change is significant in sign are represented by colour-scale values; dashed lines are superimposed if change is not significant in magnitude; grey represents areas where change is not significant in both magnitude and sign [Colour figure can be viewed at wileyonlinelibrary.com]

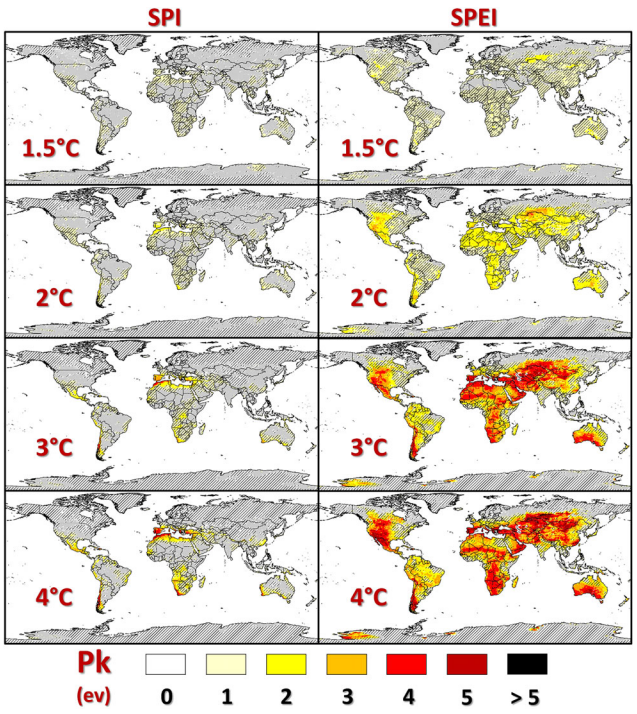

FIGURE 2 Number of events (over each 30-year period corresponding to the GWLs) more severe (PK) than the most severe one occurred in 1981–2010, according to SPI and SPEI. Grey represents areas where at least two-thirds of the simulations project 0 PK, otherwise they are represented by colour-scale values. Dashed lines are superimposed if the number of PK is projected by less than two-thirds of simulations [Colour figure can be viewed at wileyonlinelibrary.com]

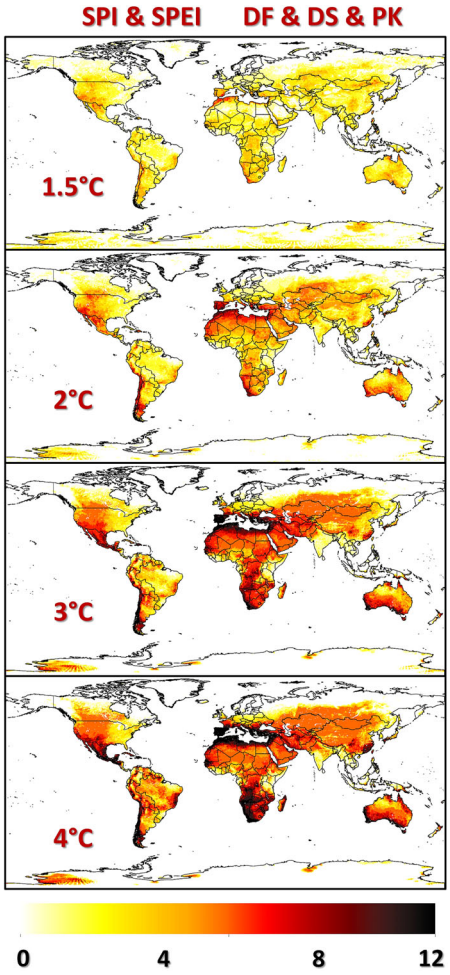

FIGURE 3 Spatial distribution of overall drought hazard score at different GWLs by combination of drought indicators (SPI-12 and SPEI-12) and the drought parameters used in this study (drought frequency, severity, and number of unprecedented events) [Colour figure can be viewed at wileyonlinelibrary.com]

The second question addresses the future occurrence of unprecedented extreme droughts (PK). The patterns of PK (Figure 2) are related to those of DF (and DS): for SPI, approximately 33% of the World is likely to experience unprecedented events starting from 1.5°C warming (Figure S9); for some areas (Chile, western Mediterranean region, and South Africa), the projections of unprecedented droughts (compared to 1981–2010) are robust already at GWL 2°C. Under higher GWLs, robust projections show up to 4 and 5 unprecedented droughts (in the 30-year period) over Chile, the Mediterranean region, southwestern South Africa, and southwestern Australia. For SPEI, approximately 75% of the World is likely to experience at least one unprecedented drought at GWL 2°C or higher, and at least three of such events over 67% of the World at GWL 4°C (Figure S10). Robust

TABLE 2 Areas (%) projected to see a significant increase in DF, DS, and PK according to both SPI and SPEI from 1981 to 2010 to four GWLs. See Figure S2 for localization of regions

Region	ALL	ALL	ALL	ALL
ALA	0.0	0.0	0.0	0.0
NEC	0.0	0.0	0.0	0.0
GIC	0.0	0.0	0.3	0.3
NWN	0.0	0.0	0.0	0.0
SWN	0.1	0.2	0.0	11.9
CNA	0.2	0.3	0.0	2.9
ENA	0.0	0.0	0.0	0.1
CAM	0.6	4.7	34.7	65.3
CAR	0.0	10.6	43.0	68.5
NWS	0.1	2.9	7.1	13.8
SAM	0.1	0.0	0.2	1.3
SSA	0.6	10.1	28.0	43.6
SWS	20.4	69.3	75.7	77.7
SES	0.1	1.9	3.5	5.0
AMZ	0.0	0.0	0.2	3.2
NEB	0.4	1.1	1.4	10.2
NEU	0.0	0.0	0.0	0.0
CEU	0.0	0.0	1.1	2.2
MED	14.3	53.5	85.9	91.5
SAH	0.5	5.9	15.3	18.4
WAF	0.1	1.1	4.9	7.8
NEAF	0.0	0.2	0.7	0.9
CEAF	0.0	0.0	1.1	0.8
SWAF	5.2	16.9	44.1	83.1
SEAF	0.3	1.8	12.7	42.8
CAF	0.0	0.2	7.4	11.1
NEA	0.0	0.0	0.0	0.0
NWA	0.0	0.0	0.0	0.0
WAS	0.0	0.2	6.2	8.7
CAS	0.0	0.0	0.4	2.2
TIB	0.0	0.0	0.0	0.0
EAS	0.1	0.8	1.0	8.0
SAS	0.2	0.1	0.0	0.7
SEA	1.0	2.5	3.7	6.1
NAU	1.1	4.6	6.0	11.5
SAU	1.5	12.4	32.6	40.2
ANT	0.1	0.0	0.0	0.1
ARCO	0.0	0.0	0.0	0.0
WORLD	1.1	4.7	9.5	14.4

projections of more than three unprecedented droughts are visible over the United States, Mexico, Chile, large parts of Africa, central Asia, and Australia at 3 and 4°C, with only the high latitude regions and part of South-East Asia and New Zealand not projected to face unprecedented droughts. Macro-regional statistics for DF, DS, and PK are reported in Tables S4 and S5.

The drought hazard projections discussed here generally agree with those reported by Zhao and Dai (2017), Spinoni *et al.* (2020), and Ukkola *et al.* (2020), but the larger number of simulations enables higher detail on transition areas such as Amazonia, central Europe, and the Sahel. The most relevant exception refers to southeastern Asia, where—according to seasonal rainfall projections discussed in Tangang *et al.* (2020) and Supari *et al.* (2020)—Indonesia is projected to face drying tendency in summer and autumn. Contrary to previous studies, which generally focused on long-time horizons (such as the end of the 21st century), our study shows that DF and DS can significantly increase even at low GWLs. This is of crucial importance in highly productive regions as China, where overall losses due to droughts can substantially increase even from GWL 1.5°C to GWL 2°C (Su *et al.*, 2018).

Combining the results of single drought variables, Figure 3 shows areas likely to be subjected to more frequent, severe, and/or unprecedented events at different GWLs. We assigned a score to the increase of each quantity (DF, DS, and PK) for each single indicator (SPI and SPEI): 0 if there is no increase, 1 if there is a significant increase in sign, and 2 if the increase is robust. Therefore, the score ranges from 0 (no increase for any category and indicator) to 12 (robust increase for all categories and indicators. Already at GWL 1.5°C, most land areas are likely to experience an increase in at least one

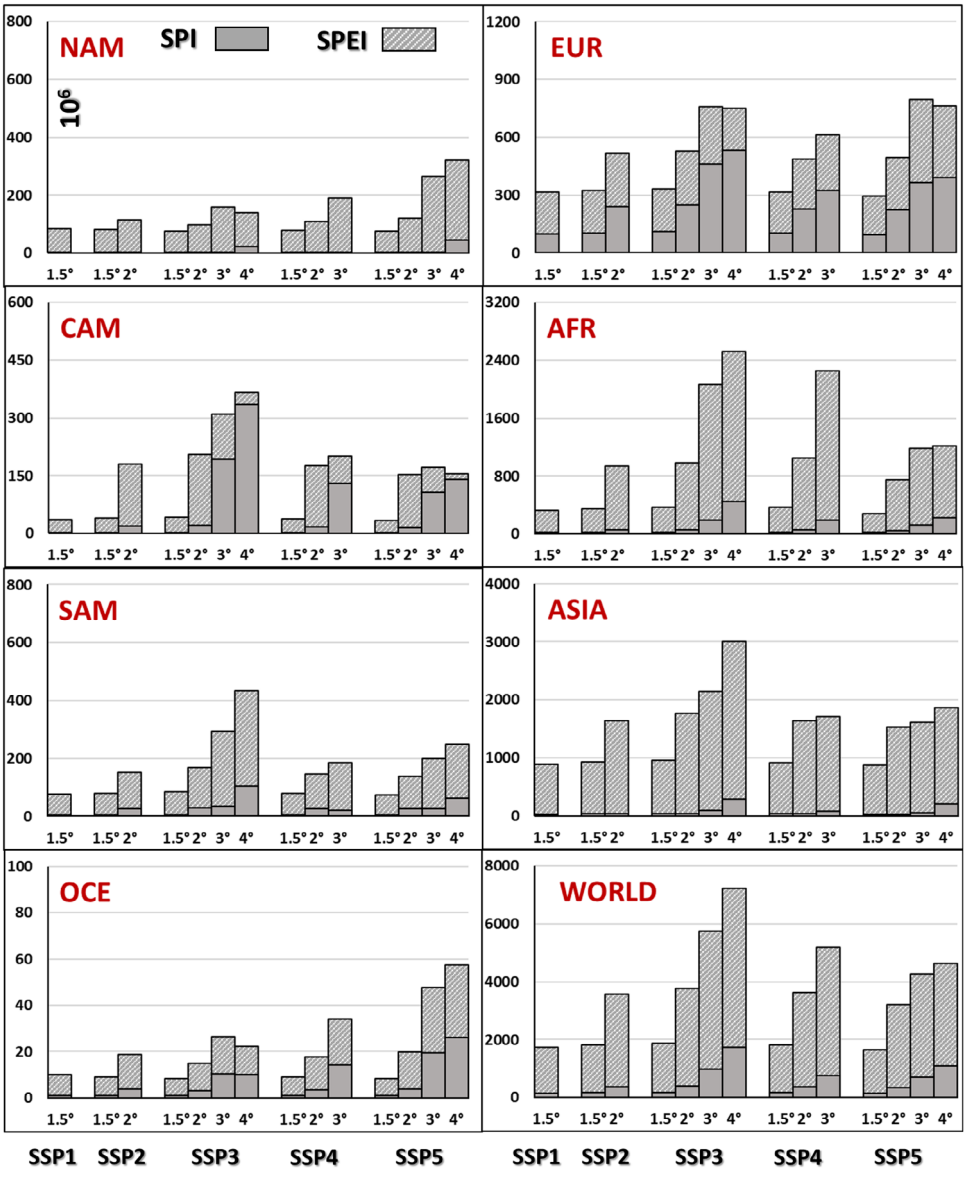

FIGURE 4 Total population (in million units) exposed to significant increase of both DF and DS for a combination of SSPs and GWLs. Values are shown for both SPI (full columns) and SPEI (dashed). Vertical scale is largely variable between the different regions due to very different population values. NAM is for North America, CAM for Central America, SAM for South America, EUR for Europe, AFR for Africa, ASIA for Asia, and OCE for Oceania. See Figure S2 for details on continents and macro-regions [Colour figure can be viewed at wileyonlinelibrary.com]

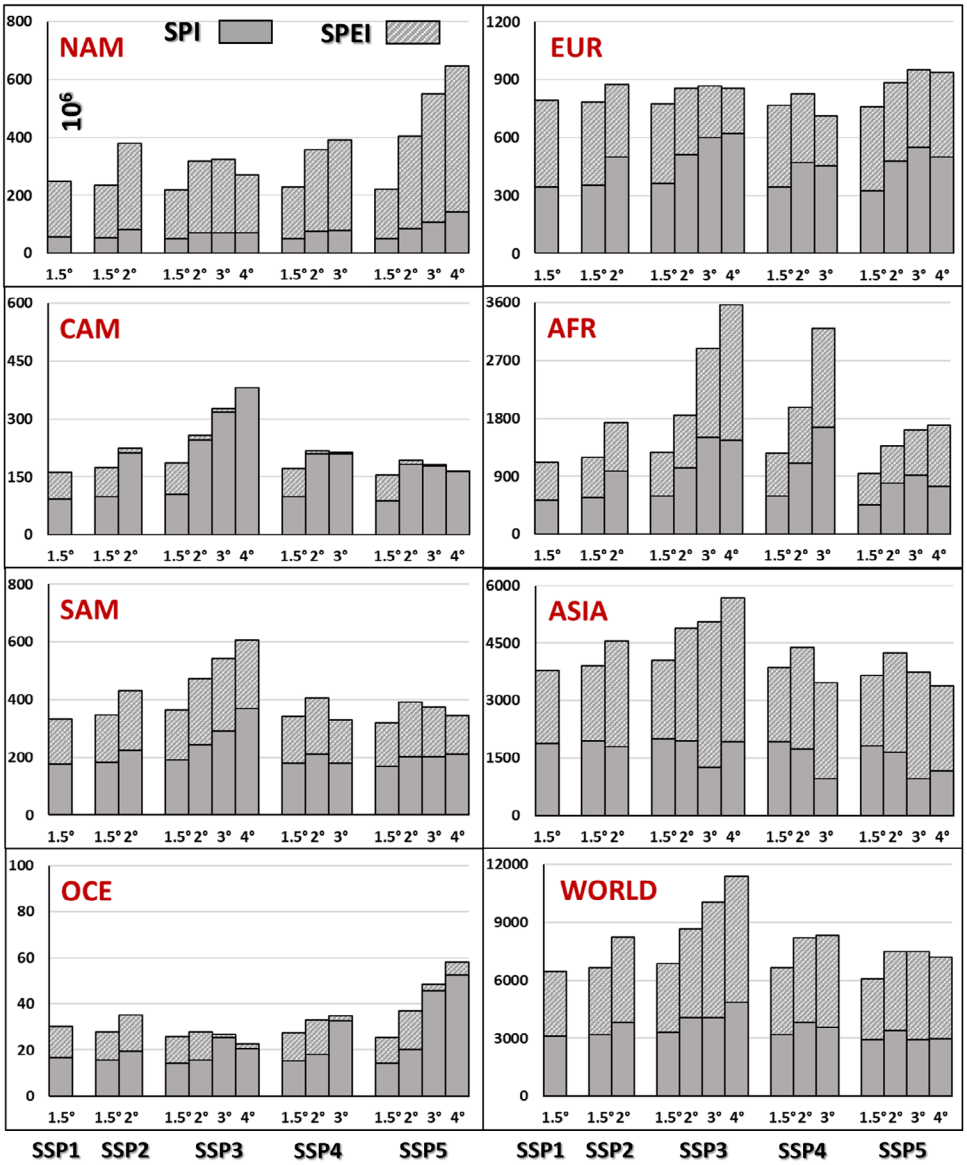

FIGURE 5 Total population (in million units) significantly exposed to at least one unprecedented event for a combination of SSPs and GWLs. Values are shown for both SPI (full columns) and SPEI (dashed) [Colour figure can be viewed at wileyonlinelibrary.com]

drought variable. At higher GWLs, drought hotspots (regions with the highest total score) become evident over Central America, Chile and southern Argentina, the Mediterranean region, the Atlantic region of Western Africa and southern Africa, southeastern China, and the western and southern coastal areas of Australia.

Figure S11 shows at which GWL some areas are projected to experience an increase—compared to 1981–2010—in DF, DS, and PK for both SPI and SPEI (thus, not necessarily caused by the temperature increase). This is likely to occur at GWL 1.5°C for the western Mediterranean and southwestern Africa, while for Yucatan (Mexico), eastern Brazil, Zambia, Zimbabwe, and parts of southeastern China it is likely to occur only if 4°C warming is reached. At macro-regional scale (Table 2), no region is likely to face an increase in DF, DS, and PK for both SPI and SPEI over more than 50% of its territories at GWL 1.5°C, but such threshold is reached by southwestern South America and the Mediterranean region at GWL 2°C and by Central America, the Caribbean Islands, and southwestern Africa at GWL 4°C. Over cold and very cold regions, less than 1% of grid points are likely to see a combined increase in DF, DS, and PK, for both the SPI and SPEI under any GWL.

3.2 | Future population exposure to droughts

When estimating the impacts on population and land-use, several combinations of SSPs, GWLs, drought indicators, and derived hazard quantities are possible: therefore, we first focus on the highest GWL compatible with each SSP, whereas other possible combinations are

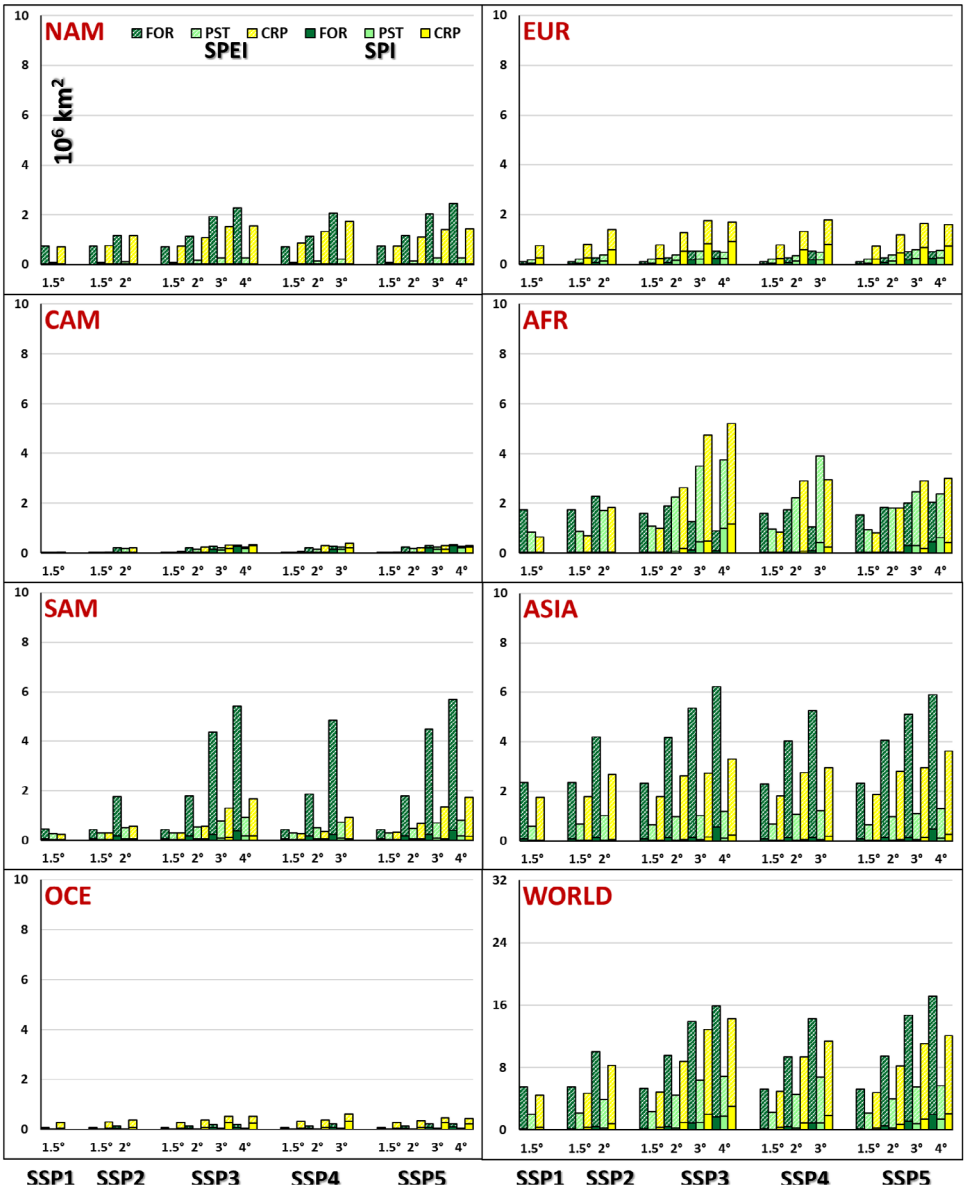

FIGURE 6 Forests (FOR), pastures (PST), and croplands (CRP), expressed in million km^2, exposed to a significant increase of both DF and DS for a combination of SSPs and GWLs. Values are shown for both SPI (full columns) and SPEI (dashed) [Colour figure can be viewed at wileyonlinelibrary.com]

discussed later. Figure 4 shows the total population at continental and global scale exposed to an increase in both DF and DS (compared to 1981–2010) under the four GWLs. Generally, for every combination of GWL and SSP, the use of SPEI results in larger values of exposed population than when using SPI: for instance, the increase in exposed population goes from around 150 million at 1.5°C to 350 million at 2°C when using SPI, but from 2 billion to nearly 4 billion with SPEI. These results are similar with all compatible SSPs.

At high GWLs, however, the choice of SSP plays a more important role. SSP3 (regional rivalry) leads to the largest values of exposed population for Central and Southern America, Africa (comparable to SSP4), and Asia, while SSP5 (fossil-fuelled development) leads to the largest values in North America, Europe (comparable to SSP3), and Oceania.

With SSP1 (green growth), less than 5% (25%) of population (in all continents) is projected to be exposed to a significant increase in DF and DS according to SPI (SPEI) (Figure S12 and Table S6 and S7). Such values increase to more than 50% of the population in Central America, Europe, and Oceania under 2°C warming with SSP2 (middle-of-the-road scenario) and when considering SPEI. With SSP4 (deepening inequality), at 3°C, population shows non negligible values also for SPI and, for SPEI, more than half of the population worldwide (excluding Asia) is likely to be exposed to a significant increase of DF and DS in all continents.

With severe SSPs (SSP3 and SSP5), the total population exposed could be very high also for SPI: with SSP3 at 3°C warming and SSP5 at 4°C warming more than 1 billion people are likely to be exposed to a significant increase in DF and DS at global scale. Such values

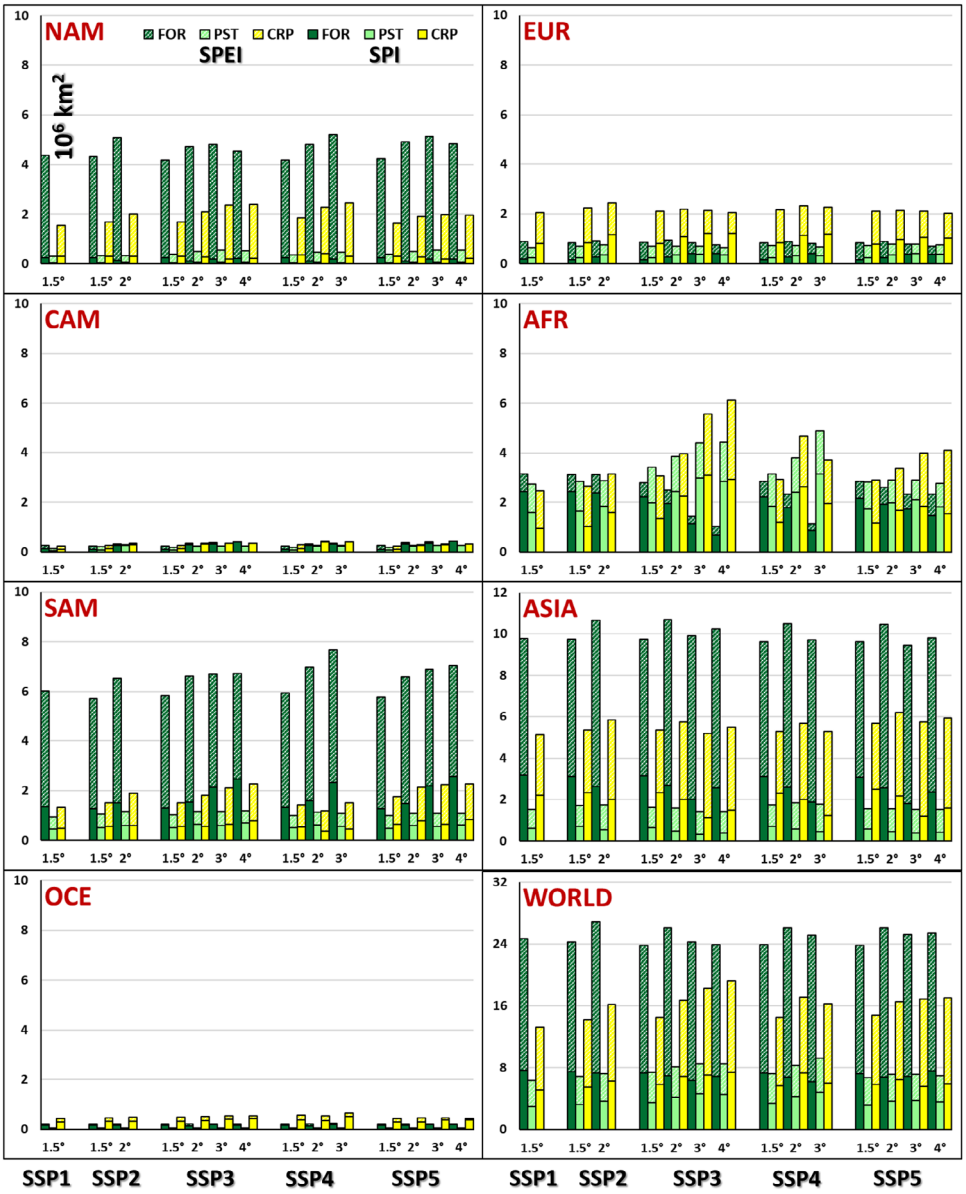

FIGURE 7 Land-use forests, pastures, and croplands, expressed in million km^2, significantly exposed to at least one unprecedented event for a combination of SSPs and GWLs. Values are shown for both SPI (full columns) and SPEI (dashed) [Colour figure can be viewed at wileyonlinelibrary.com]

correspond to approximately 10 and 14% of global population with SSP3 (respectively, at 3 and 4°C) and 15% with SSP5 at 4°C warming. According to SPEI, such exposure goes above 4 billion people at GWL 3°C with SSP3 (about 55%), SSP4 (close to 60%), and SSP5 (about 53%) and, in every continent, more than 40% of population is likely to see a significant increase of DF and DS at GWL 4°C with SSP3 or SSP5, with a value of more than 7 billion people reached with SSP3 at GWL 4°C.

Projected exposure to at least one drought more severe than those observed in 1981–2010 is shown in Figure 5. Focusing at the worst-case combination of SSPs and GWLs, results show that more than 11 billion people (i.e., more than 90% of global projected population) are likely to be exposed to such unprecedented events with SSP3 at 4°C, mainly in Asia (close to 6 billion) and Africa (more than 3.5 billion). It is important to note that such large values (peaking with SSP3 for Central and South America, Africa, and Asia, and with SSP5 for North America and Oceania) are a consequence of the expected increase in population, rather than drought hazard. In fact, in terms of fraction of total population exposed, results show (Figure S13 and Tables S8 and S9) large values already at 1.5° C (around 40% with SPI and more than 80% with SPEI, excluding North America), with more than 90% of population exposed to the occurrence of unprecedented events with all SSPs and for most continents at 2°C warming.

3.3 | Future land-use exposure to droughts

Figure 6 shows the land-use exposure to increased DF and DS: in absolute values, forests represent the most

exposed class in North and South America, and Asia, croplands in Europe and Oceania, independently of the SSP. In Africa, on the other hand, forests are the most affected class with SSP1 and SSP2, croplands with SSP3 and SSP5, and pastures with SSP4. The use of SPEI generally results in much larger exposed values, especially at high GWLs for all land-use classes considered and, for example, for forests at the global scale, the exposure with SPEI can reach values 8 times larger than with SPI. Looking at percentages (Figure S14), pastures become the most affected class at global scale in any SSP from 2°C warming and in some continents (Central and South America, Africa, and Oceania) all land-use classes show exposure larger than 60% from 3°C warming.

The SSP does not play a decisive role at 1.5 and 2°C for any land-use classes (and, for forests, even at 3°C) but pastures and croplands show the largest values under SSP4 and SSP3 at 3°C, respectively. At 4°C, forests show the largest exposed values under SSP5, while croplands and pastures under SSP3 for both indicators.

In a World which follows a green growth (SSP1), less than 5% of land-use classes are projected to be exposed to a significant increase in DF and DS according to SPI, while for SPEI such values are generally below 25%, but could be close to 30% for pastures and croplands. With SSP2 (middle-of-the-road) and at GWL 2°C, land-use shows limited exposure for SPI, but for SPEI the exposed fractions are above 50% in Central America, Europe (excluding forests), Africa, and Oceania.

With a development based on deepening inequality (SSP4), the progressive increase of exposure is evident and, at 3°C, all categories show non-negligible values also for SPI (excluding North America). With SSP4 and SPEI, more than half of pastures and croplands are projected to be exposed to a significant increase of DF and DS in all

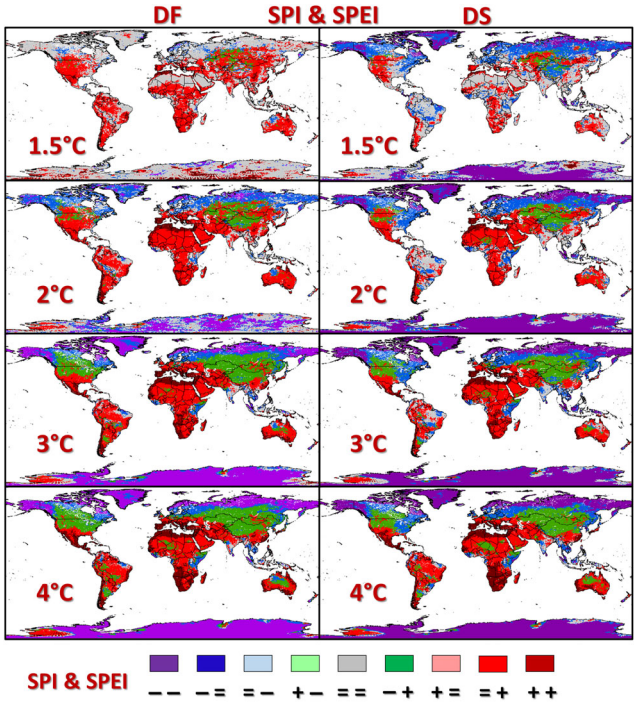

FIGURE 8 Concordance between SPI and SPEI on tendencies of drought frequency (DF) and severity (DS). Red-like areas represent significant increase for at least one indicator, blue-like significant decrease for at least one indicator, grey-like no significant change, green-like opposite tendencies [Colour figure can be viewed at wileyonlinelibrary.com]

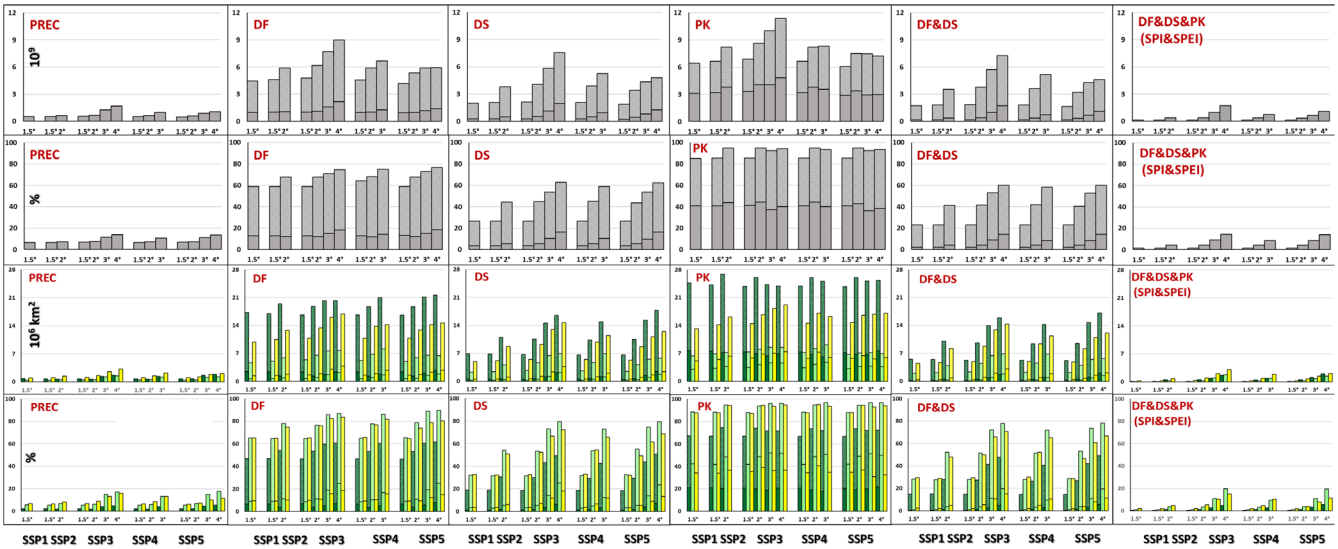

FIGURE 9 Global population (first row: billion units, second row: %) and land-use (first row: million km^2, second row: %) exposed to significant drying and increase of drought quantities for a combination of GWLs and SSPs [Colour figure can be viewed at wileyonlinelibrary.com]

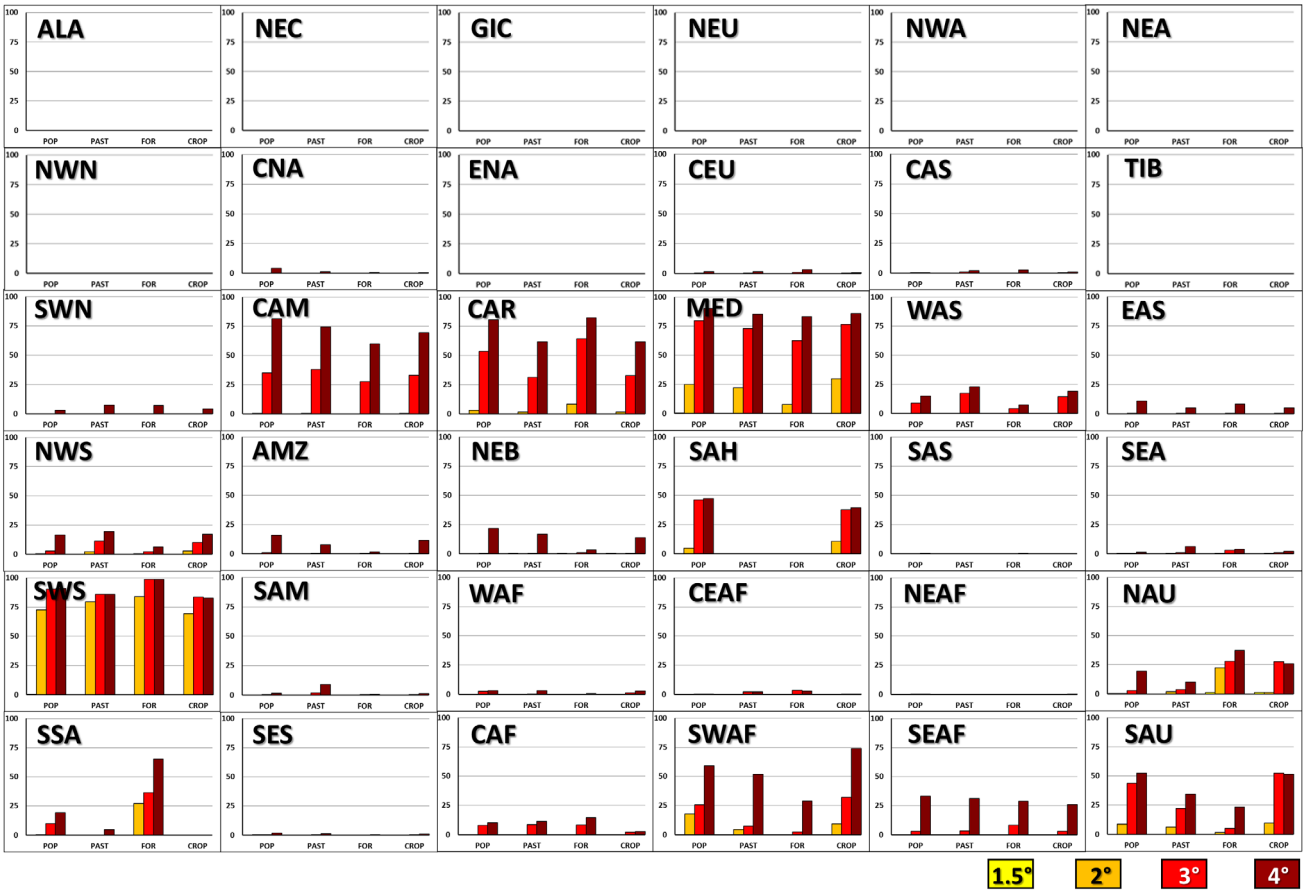

FIGURE 10 Percentage of areas with population and land-use exposure to significant increase in DF, DS, and PK for both SPI and SPEI at different GWLs under the SSP5 scenario. See Figure S2 for definition of regions [Colour figure can be viewed at wileyonlinelibrary.com]

FIGURE 11 Population and land-use progressive exposure to significant increase of both DF and DS at different GWLs under the SSP5 scenario, according to SPI (left) and SPEI (right). White represents areas with population below 1 inhabitant/km^2 and land-use below 5% over the grid point [Colour figure can be viewed at wileyonlinelibrary.com]

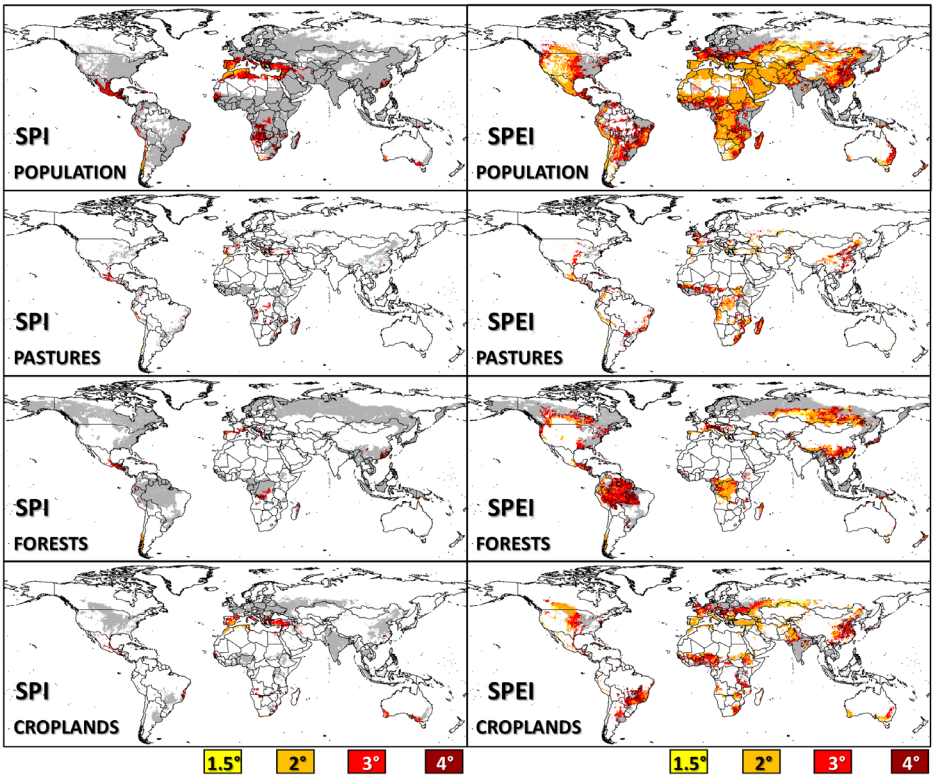

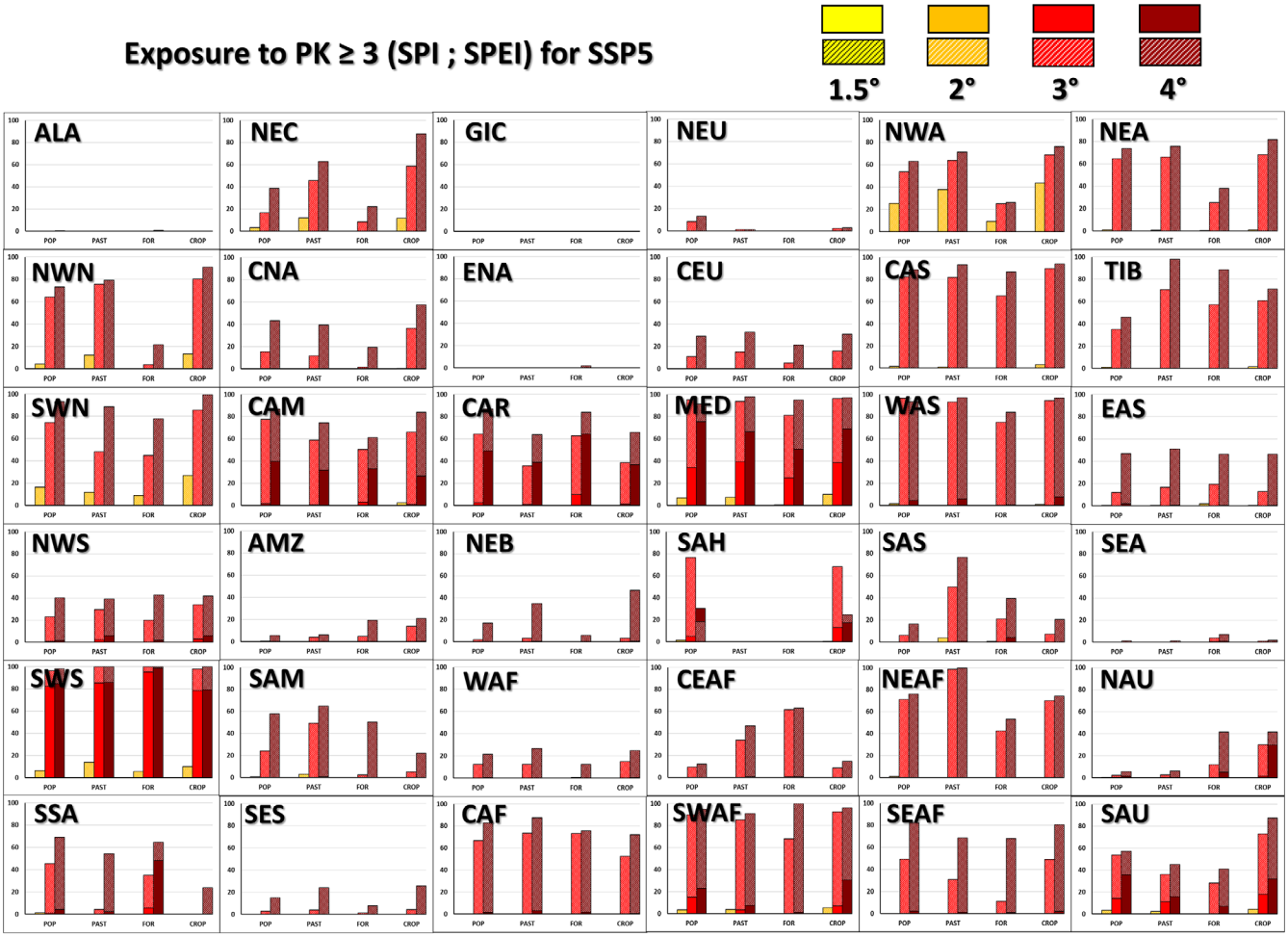

FIGURE 12 Percentage of population land-use areas exposed to at least 3 unprecedented drought events for SPI (non-dashed columns) and SPEI (dashed columns) at different GWLs under the SSP5 scenario [Colour figure can be viewed at wileyonlinelibrary.com]

continents at GWL 3°C. With severe SSPs (SSP3 and SSP5) and according to SPEI, in every continent more than 40% of croplands are projected to experience a significant increase of DF and DS at GWL 4°C, and such fraction is even larger for pastures (>60%, excluding North America). Instead, in North America and Europe forests show exposure values below 40% even with SSP3 and SSP5, and in Asia such values are just above 40% at GWL 4°C.

The saturation effect described for population is also visible for land-use classes exposed to unprecedented droughts (Figure 7 and Figure S15): with SPEI, pastures and croplands show significant exposure values larger than 80% almost in every continent under all SSPs and GWL 1.5°, and forests are below 60% of exposure only in North America and Europe, but never below 40%. With SPI, such values are smaller, but in some continents they show very large values (e.g., pastures and croplands in Central America and Oceania) and, at global scale, they are around 20% for forests (60% with SPEI), 35% for croplands (90% with SPEI), and 45% with pastures (95% with SPEI). Moving to absolute values, the saturation effect is still evident for forests (total exposure of 24–26 million km^2 with SPEI and 7–8 million km^2 with SPI) and pastures (7–10 million km^2 with SPEI and 4–6 million km^2 with SPI), while croplands show values that generally depend more on the GWL than on SSP, peaking at GWL 4°C with 19 million km^2 exposed under SSP3 (with SPEI).

3.4 | The importance of temperature in drought hazard and exposure

Although climate models consistently project a progressively warmer 21st century, precipitation projections are spatially heterogeneous, with a small global average increase, a wetting tendency over high latitudes in the Northern Hemisphere, tropical Africa and Pacific Asia, and drying over Mexico, Chile, the Mediterranean

TABLE 3 Global population (10^6 inhabitants) and land-use (10^6 km^2) exposed to a significant (and robust) increase in drought quantities from 1981 to 2010 to the highest GWL for each SSP, according to SPI and SPEI

	SSP (GWL)		SSP1	(1.5°)			SSP2	(2°)			SSP3	(4°)			SSP4	(3°)			SSP5	(4°)	
	IND/CLASS	POP	PST	CRP	FOR	POP	PST	CRP	FOR	POP	PST	CRP	FOR	POP	PST	CRP	FOR	POP	PST	CRP	FOR
	SPI_DF (M)	989.4	0.6	1.4	2.4	1,054.7	0.8	1.8	1.4	2,183.9	2.2	3.8	2.4	1,287.9	1.6	2.8	1.7	1,421.4	1.8	2.7	2.7
	SPEI_DF (M)	4,462.2	4.7	9.8	17.2	5,873.2	5.9	12.8	19.5	9,002.6	7.7	16.9	20.2	6,674.5	8.2	14.2	21.0	5,924.9	6.5	14.6	21.6
	SPI_DS (M)	263.5	0.2	0.5	0.5	484.9	0.4	1.1	0.7	1962.5	2.2	3.7	2.1	924.4	1.2	2.1	1.2	1,256.0	1.7	2.4	2.5
	SPEI_DS (M)	2005.9	2.3	4.9	6.9	3,835.2	4.1	8.7	11.0	7,576.2	7.0	14.7	16.5	5,247.8	6.9	11.5	14.9	4,817.0	5.8	12.5	17.7
Significant	SPI_PK (M)	3,090.4	3.0	5.2	7.7	3,802.4	3.7	6.3	7.3	4,842.4	4.6	7.4	6.9	3,564.3	4.8	6.0	6.2	2,976.4	3.6	5.9	7.6
	SPEI_PK (M)	6,464.4	6.3	13.2	24.7	8,226.9	7.2	16.2	26.9	11,374.3	8.5	19.2	23.9	8,333.9	9.2	16.3	25.1	7,217.2	7.0	17.1	25.3
	SPI_DFDS (M)	156.1	0.1	0.3	0.2	372.8	0.3	0.8	0.5	1736.1	1.8	3.1	1.7	762.5	0.9	1.8	0.9	1,093.4	1.4	2.1	2.0
	SPEI_DFDS (M)	1742.4	2.0	4.5	5.5	3,559.5	3.9	8.3	10.0	7,238.4	6.9	14.3	15.9	5,180.9	6.8	11.4	14.2	4,625.3	5.7	12.1	17.1
	ALL (M)	123.5	0.1	0.3	0.2	372.8	0.3	0.8	0.5	1735.9	1.8	3.1	1.7	762.2	0.9	1.8	0.9	1,093.3	1.4	2.1	2.0
	SPI_DF (M)	1.5	0.0	0.0	0.0	107.1	0.1	0.3	0.2	1,593.7	1.3	2.8	1.4	675.1	0.5	1.5	0.8	997.4	1.1	1.9	1.6
	SPEI_DF (M)	137.5	0.1	0.3	0.4	2021.4	1.8	5.0	4.0	7,338.6	6.8	14.4	15.8	4,915.3	6.4	10.9	13.8	4,691.5	5.6	12.1	16.9
	SPI_DS (M)	2.3	0.0	0.0	0.0	75.5	0.1	0.2	0.0	1,286.8	1.3	2.6	1.1	342.4	0.3	1.0	0.4	776.6	1.0	1.6	1.4
	SPEI_DS (M)	59.5	0.1	0.4	0.3	1,126.4	0.9	3.0	2.3	5,966.7	5.9	12.0	12.8	3,541.2	4.6	7.8	7.1	3,722.2	4.8	9.9	13.8
Robust	SPI_PK (M)	183.0	0.2	0.5	0.4	824.1	0.7	1.6	1.5	2,942.2	3.1	4.9	3.8	1,628.9	2.5	3.1	2.5	1856.4	2.5	3.4	4.3
	SPEI_PK (M)	2061.6	2.7	5.4	7.8	5,628.2	5.7	12.4	17.7	10,185.4	8.0	17.9	21.2	6,933.2	8.4	14.4	21.3	6,467.0	6.6	15.7	22.6
	SPI_DFDS (M)	0.0	0.0	0.0	0.0	57.5	0.0	0.2	0.0	1,083.5	0.8	2.1	0.8	302.4	0.2	0.9	0.3	662.3	0.7	1.4	1.0
	SPEI_DFDS (M)	7.4	0.0	0.0	0.0	918.8	0.6	2.5	1.3	5,632.8	5.7	11.3	11.3	3,373.1	4.3	7.5	6.5	3,482.8	4.6	9.3	12.3
	ALL (M)	0.0	0.0	0.0	0.0	57.5	0.0	0.2	0.0	1,082.5	0.8	2.1	0.8	302.4	0.2	0.9	0.3	661.8	0.7	1.4	1.0

Region, southwestern Africa and southern Australia (-Figure S6 and Table S5). Regarding drought hazard, the choice between SPI or SPEI results in differences in future DF (Figure 1), DS (Figure S7), and PK (Figure 2 and Figure S9–S10) that are almost negligible at GWL 1.5°C, start to emerge at GWL 2°C, and become progressively larger at GWLs 3 and 4°C, due to pronounced temperature increases under extreme climate scenarios in the second half of the 21st century (IPCC, 2014). In the Northern Hemisphere, we note regions with opposite tendencies, depending on the drought indicator, for both DF and DS (green areas in Figure 8), where a precipitation decrease is overbalanced by the temperature increase: Asia from 2°C and North America from 3°C. In the Southern Hemisphere, this occurs for very limited (at 3°C) or limited (at 4°C) areas, specifically over central-western Brazil and central Argentina, central Australia. See Figures S16 and S17 and Table S8 for macro-regional statistics.

Remarkable differences between the two drought indicators can, therefore, be found in population and land-use projected exposure to drought events. In particular, the use of temperature as a drought driver (in this case with SPEI) can be dominant over areas with unclear precipitation projections, for example, over North America, where population exposed to an increase of both DF and DS at 4°C ranges between ∼10% when using SPI to ∼50% for SPEI (Figure S12). Population and land-use (Figure 9) show larger exposure to every drought-derived quantity with SPEI than with SPI. For example, the global population exposed to a significant increase in DF is about four to five times larger with SPEI than with SPI in all SSPs (Table 3 and Table S19). Larger differences are found by comparing the exposure to a significant increase in DS and slightly smaller by comparing the significant exposure to unprecedented events.

Focusing on simultaneous significant increases of DF and DS, the combination leading to the largest exposure, at global scale, is met with SSP3 at 4°C (excluding forests with SSP5 at 4°C) for both indicators (Figure 9). However, if we focus on severe SSPs (SSP3, SSP4, and SSP5), according to SPI the exposure of each category never exceeds 20%, while with SPEI it is never below 40%. About unprecedented droughts, if we base our analyses on precipitation (SPI), the global exposure of population is ∼40% for all SSPs, ∼20% for forests, ∼35% for croplands, and 50% for pastures; including also temperature (SPEI), such values increase to the point that at least 60% of forests and 80% of population, pastures, and croplands are exposed to PK ≥1 at the highest GWL of any SSP.

Other than the clear effect of temperature, Figure 9 shows that, using SPI, population and land-use exposure to a significant increase in DS is similar—in terms of total numbers—to that related to a significant precipitation decrease, while the exposure related to significant increases in DF and PK is instead larger. This highlights the role of precipitation variability in drought projections, which can be more important than mean changes. Climate change is known to cause a higher frequency of extreme precipitation events (Giorgi *et al*., 2019) and enhanced interannual precipitation variability (e.g., Giorgi and Bi, 2005) and this likely occurs also for droughts as, due to the increased variability, regions projected to face a long-term decrease in overall precipitation could face an increase in DF and experience extreme events never recorded in the past (IPCC, 2018).

Depending on drought indicators, the differences in exposure to drought tend to become larger with increasing GWL, which is expected as the SPEI includes temperature. However, this could raise questions about a possible overestimation of drought trends by SPEI due to overestimation of PET, in particular over drylands (Weiss and Menzel, 2008). Thus, we investigated population and land-use exposed to simultaneous significant increases in DF, DS, and PK for both SPI and SPEI (rightmost panels in Figure 9 and Table S12). The results show that including temperature in meteorological drought projections can indeed exaggerate some drought patterns, especially in the second half of the 21st century under more severe combinations of climate and socio-economic scenarios, especially over humid regions where a robust increase in temperature is not associated with counterpart significant drying. Consequently, as specific sectors potentially affected by drought could require different types of drought indicators, depending on the type of risk one wants to quantify, we suggest performing analyses on exposure to drought hazard by using combinations of indicators that include and neglect temperature.

3.5 | Focusing on fossil-fuelled scenario (SSP5)

Because RCP8.5 allows reaching extreme warming levels (Riahi *et al*., 2011), it can be used to analyse worst-case scenarios for drought hazard (Spinoni *et al*., 2020). For this reason, and because SSP5 is best coupled with RCP8.5 (O'Neill *et al*., 2016), which includes the largest number of simulations used in this study (54%), here we specifically focus on the combination SSP5-RCP8.5 (not misled with SSP5-8.5; Wyser *et al*., 2020). The SSP5 foresees a future rapid economic growth associated with unrestricted carbon-based energy use (van Vuuren *et al*., 2011a; Leimbach *et al*., 2017). It implies high mitigation challenges and relatively low challenges in adaptation: the technological progress aims at strong

development at the cost of huge exploitation of fossil-fuel energy, and therefore very high CO_2 emissions (Kriegler *et al*., 2017). With SSP5, population—subjected to massive urbanization—shall peak around the mid-2050s and subsequently decline close to current values, especially over east Asia (Samir and Lutz, 2014; Jones and O'Neill, 2016).

Results for simultaneous population and land-use exposure to increased DF, DS, and PK agreed by both SPI and SPEI are shown in Figure 10. Many regions show small or negligible exposed fractions for all categories and GWLs, especially above 45°N and at tropical latitudes in Africa and Asia. Instead, regions with not negligible exposed population and land-use at GWL 2°C generally show a progressive exposure increase with increasing GWL. If we arbitrarily define as drought hotspots (under SSP5) the macro-regions with at least 20% of population, pastures, forests, and croplands exposed to the worst drought conditions, southwestern South America becomes hotspot at GWL 2°C, Central America, the Caribbean, and the Mediterranean Region at GWL 3°C, and southwestern Africa, south-eastern Africa, and southern Australia at GWL 4°C.

The key role of temperature is undeniable also within SSP5: population and land-use are likely to be widely exposed to a significant increase in DF and DS (Figure 11) over most of the regions at GWL 3°C warming according to SPEI, while this occurs at GWL 4°C and over few regions for SPI. Other than the extent of areas (much wider using SPEI), the effect of temperature (so the use of SPEI) allows the identification of progressive exposure over all continents (Figure 11, right panels), while for the SPI this occurs only over Central America, the Mediterranean region, and sparse areas elsewhere. For pastures, the most evident differences between SPI and SPEI are in sub-Saharan Africa and northeastern China. In addition, the use of SPEI shows the evolution of drought effects on boreal forests in Canada and Russia and the tropical forests of Amazonia, the Congo river basin, and southern China, along with extended croplands at mid-latitudes in Central United States, Europe, and eastern China, as well as over centre-eastern Brazil, northeastern Argentina, equatorial Africa, south-eastern South Africa, and parts of India and Pakistan.

The role of temperature is also clear at the continental scale: for example, in North America for SPI, significant fractions of population and land-use are exposed to an increase in DF and DS only at GWL 3°C and only in southern Mexico, whereas for SPEI, population is already exposed to a significant increase in DF and DS over sparse areas in the United States and Mexico at GWL 1.5°C, progressively extending to southern Canada, most of the United States, Mexico, and the Caribbean. In addition, differently than for SPI, forests are projected to be progressively exposed in Canada and the northwestern United States and croplands over most of the Mississippi river basin when using SPEI.

We also investigated which regions are likely to be hit by at least three unprecedented drought events in the SSP5 case (Figure 12). Only a few very cold (Alaska, northeastern North America, Greenland and Iceland, and northern Europe) and very humid (Amazonia and southeastern Asia) regions show significant exposure values below (or close to) 20% for all categories and GWLs. According to SPI, only southwestern South America and the Mediterranean region (at 3°C), and Central America and the Caribbean (at 4°C) show significant exposure larger than 20% for population and land-use. According to SPEI, in 15 (out of 36) macro-regions, more than 20% of population and land-use classes will face at least three unprecedented events at 3 and, at 4°C, such regions are 25, representing more than 50% of lands.

4 | CONCLUSIONS

This study builds on a previous paper (Spinoni *et al*., 2020), which focused on GCM and RCM based meteorological drought hazard projections for the end of the 21st century. Here, we extend the analysis to population and land-use exposure to future drought events under a combination of GWLs and SSPs. Overall, the drought hazard increases with increasing GWL and more frequent and severe events are projected over large areas of the world, in particular when using the SPEI as drought indicator (Figures 1–3). A few drought hotspots can be identified: Central America, southwestern South America, the Mediterranean Region, southern Africa, southeastern China, and southern Australia. Most of these hotspots were also noted by Lehner *et al*. (2017), Carrão *et al*. (2018), and Spinoni *et al*. (2020), and recent studies reported on future worsening of drought conditions in Central United States and Mexico (Wehner *et al*., 2011; Cook *et al*., 2015), southern South America (Penalba and Rivera, 2013); southern Europe (Spinoni *et al*., 2018), and different parts of Africa (Ahmadalipour *et al*., 2019). The largest increases in drought hazard are likely to occur over regions already vulnerable to this hazard (Carrao *et al*., 2016), which could consequently have adverse impacts on social and ecological systems (Steffen *et al*., 2015).

Population and land-use exposure to droughts increases depending on both GWL and SSP (Figures 4 and 5). As reported by Smirnov *et al*. (2016) for population, exposure shows small variations with SSPs at

moderate GWLs, while at 3 and 4°C the differences become larger. According to SPI, population and land-use exposure to drought events is limited in a World following a more sustainable development and not exceeding 2°C of global warming (SSP1 and SSP2) while, according to SPEI, both population and land-use exposure to droughts is remarkable already with these SSPs, and not only with the more severe ones (SSP3, SSP4, and SSP5), where 3 and 4°C are reached. Globally, around 2 billion people are likely to be exposed to increased DF and DS (around 5 billion to unprecedented events) when using SPI with any SSP, while with SPEI such values are significantly larger (respectively, 3 and 7 billion people), except with SSP1 (Figure 9 and Table 3).

The feedbacks induced by global warming and drought stress are known to reduce plant resilience and increase forest mortality in many regions of the World (Allen *et al*., 2010), impact on crop yields (Parry *et al*., 2005; Li *et al*., 2009; Leng and Hall, 2019), and force farmers to urgent adaptation (Avery *et al*., 2008). The land-use exposed to increased DF and DS is very small or negligible with SPI but large with SPEI, especially with SSP3, SSP4, and SSP5 (Figure 6). However, relevant fractions of all land-use will face at least one unprecedented drought with both SPI and SPEI and any SSP (Figure 7), and at least three unprecedented droughts with SSP5 (Figure 12) and SSP3.

In the last decades, droughts have been increasingly aggravated by heat-waves (Zscheischler *et al*., 2018) and in some cases these phenomena are so strongly connected that excluding temperature from drought analyses could lead to an underestimation of events such as the one in Europe in 2003, which had massive impacts on population, forests, and agriculture (Haines *et al*., 2006; Rebetez *et al*., 2006), or the one over Russia in 2010, with large impacts on agriculture and ecology (Loboda *et al*., 2017). If we consider temperature (SPEI), around 50% of global lands will face an increase in DF in the 21st century while, if temperature is not included (SPI), this value stays below 10% even at 4°C. The use of temperature in drought hazard projections is of particular importance over North America and Asia, where large areas show a positive drought tendency if temperature is considered and a negative one if it is not (Figure 8). Accounting for temperature results in larger population and land-use fractions exposed to droughts with increasing GWL, also due to increased duration of future drought, other than increased frequency and severity (Figure 11).

Investigating droughts with and without temperature as a driver can be of key importance in impact assessments, especially if the effect of precipitation and temperature is considered both separately and in combination, for example on forests (Williams *et al*., 2013; Jeong *et al*., 2014; McDowell and Allen, 2015; Xie *et al*., 2015; Choat *et al*., 2018), crops (Gourdji *et al*., 2013; Zhao *et al*., 2017), and pastures (Perera *et al*., 2019). However, the potential sources of uncertainties are manifold and related to climate simulations (Knutti and Sedláček, 2013; Orlowsky and Seneviratne, 2013; Friedlingstein *et al*., 2014; Dai and Zhao, 2017), population projections (Azose *et al*., 2016), and land-use projections (Prestele *et al*., 2016).

The results of this study will be included in the European Commission's Global Drought Observatory (GDO, https://edo.jrc.ec.europa.eu/gdo/). As possible improvements, such projections could be updated when the new generation of coupled SSP-RCP simulations will be available at high resolution (Gidden *et al*., 2019), in order to reduce the uncertainties caused by the mixture of climate data based on RCPs and population and land use data based on SSPs. Moreover, other drought indicators can be investigated, for example, soil moisture, usually applied to investigate agricultural droughts (Sheffield and Wood, 2008; Berg *et al*., 2017), for croplands and pastures. For forests, the vegetation response to drought can be tested using remotely sensed data (Cammalleri *et al*., 2016), eventually considering also primary productivity (Vicente-Serrano *et al*., 2013; Xu *et al*., 2019b). Finally, as this study analyses only the hazard and exposure components of drought risk, it is also worth assessing drought vulnerability in multiple sectors (as done for Africa by Ahmadalipour *et al*., 2019), despite vulnerability to drought is difficult to quantify (Carrao *et al*., 2016), also considering single categories like forests (Choat *et al*., 2012), crops or pastures (Wilhite, 1993; Antwi-Agyei *et al*., 2012), or society (Wilhite *et al*., 2019).

AUTHOR CONTRIBUTIONS

Jonathan Spinoni: Conceptualization; data curation; formal analysis; investigation; methodology; software; supervision; validation; visualization; writing - original draft; writing-review & editing. **Paulo Barbosa:** Conceptualization; writing-review & editing. **Edoardo Bucchignani:** Data curation; writing-review & editing. **John Cassano:** Data curation; writing-review & editing. **Tereza Cavazos:** Data curation; writing-review & editing. **Alessandro Cescatti:** Data curation; writing-review & editing. **Jens Christensen:** Data curation; writing-review & editing. **Ole Christensen:** Data curation; writing-review & editing. **Erika Coppola:** Data curation; writing-review & editing. **Jason Evans:** Data curation; writing-review & editing. **Giovanni Forzieri:** Conceptualization; data curation; methodology; writing - original draft; writing-review & editing. **Beate Geyer:** Data curation; writing-review & editing. **Filippo Giorgi:** Data curation; writing-review & editing.

Daniela Jacob: Data curation; writing-review & editing. **Torben Koenigk:** Data curation; writing-review & editing. **Rene Laprise:** Data curation; writing-review & editing. **Chris Lennard:** Data curation; writing-review & editing. **M. Levent Kurnaz:** Data curation; writing-review & editing. **Delei Li:** Data curation; writing-review & editing. **Marta Llopart:** Data curation; writing-review & editing. **Niall McCormick:** Writing-review & editing. **Gustavo Naumann:** Conceptualization; methodology; writing - original draft; writing-review & editing. **Grigory Nikulin:** Data curation; writing-review & editing. **Tuğba Öztürk:** Data curation; writing-review & editing. **Hans-Jürgen Panitz:** Data curation; writing-review & editing. **Rosmeri da Rocha:** Data curation; writing-review & editing. **Silvina Solman:** Data curation; writing-review & editing. **Jozef Syktus:** Data curation; writing-review & editing. **Fredolin Tangang:** Data curation; writing-review & editing. **Claas Teichmann:** Data curation; writing-review & editing. **Robert Vautard:** Data curation; writing-review & editing. **Juergen Vogt:** Conceptualization; methodology; writing - original draft; writing-review & editing. **Katja Winger:** Data curation; writing-review & editing. **George Zittis:** Data curation; writing-review & editing. **Alessandro Dosio:** Conceptualization; data curation; methodology; writing - original draft; writing-review & editing.

ORCID

Jonathan Spinoni https://orcid.org/0000-0002-8903-085X
Tereza Cavazos https://orcid.org/0000-0003-3097-9021
Torben Koenigk https://orcid.org/0000-0003-2051-743X
Gustavo Naumann https://orcid.org/0000-0002-8767-5099
Tugba Ozturk https://orcid.org/0000-0001-8598-8596
George Zittis https://orcid.org/0000-0002-6839-5622

REFERENCES

Ahmadalipour, A., Moradkhani, H., Castelletti, A. and Magliocca, N. (2019) Future drought risk in Africa: integrating vulnerability, climate change, and population growth. *Science of the Total Environment*, 662, 672–686.

Ahmadalipour, A., Moradkhani, H. and Demirel, M.C. (2017) A comparative assessment of projected meteorological and hydrological droughts: elucidating the role of temperature. *Journal of Hydrology*, 553, 785–797.

Akinsanola, A.A. and Zhou, W. (2019) Projections of West African summer monsoon rainfall extremes from two CORDEX models. *Climate Dynamics*, 52(3–4), 2017–2028.

Allen, C.D., Macalady, A.K., Chenchouni, H., Bachelet, D., McDowell, N., Vennetier, M., et al. (2010) A global overview of drought and heat-induced tree mortality reveals emerging climate change risks for forests. *Forest Ecology and Management*, 259(4), 660–684.

Antwi-Agyei, P., Fraser, E.D., Dougill, A.J., Stringer, L.C. and Simelton, E. (2012) Mapping the vulnerability of crop production to drought in Ghana using rainfall, yield and socioeconomic data. *Applied Geography*, 32(2), 324–334.

Ashfaq, M., Cavazos, T., Reboita, M.S., Torres-Alavez, J.A., Im, E.S., Olusegun, C.F., Alves, L., Key, K., Adeniyi, M.O., Tall, M., Sylla, M.B., Mehmood, S., Zafar, Q., Das, S., Diallo, I., Coppola, E. and Giorgi, F. (2020) Robust late twenty-first century shift in the regional monsoons in RegCM-CORDEX simulations. *Climate Dynamics*. https://doi.org/10.1007/s00382-020-05306-2.

Asner, G.P., Brodrick, P.G., Anderson, C.B., Vaughn, N., Knapp, D. E. and Martin, R.E. (2016) Progressive forest canopy water loss during the 2012–2015 California drought. *Proceedings of the National Academy of Sciences*, 113(2), E249–E255.

Avery, D., Avery, F., Ogle, G.I., Wills, B.J. and Moot, D.J. (2008) Adapting farm systems to a drier future. In: *Proceedings of the New Zealand Grassland Association*, Vol. 70. Dunedin, NZ: New Zealand Grassland Association, pp. 13–18.

Azose, J.J., Ševčíková, H. and Raftery, A.E. (2016) Probabilistic population projections with migration uncertainty. *Proceedings of the National Academy of Sciences*, 113(23), 6460–6465.

Beguería, S., Vicente-Serrano, S.M., Reig, F. and Latorre, B. (2014) Standardized precipitation evapotranspiration index (SPEI) revisited: parameter fitting, evapotranspiration models, tools, datasets and drought monitoring. *International Journal of Climatology*, 34(10), 3001–3023.

Below, R., Grover-Kopec, E. and Dilley, M. (2007) Documenting drought-related disasters: a global reassessment. *The Journal of Environment & Development*, 16(3), 328–344.

Berg, A., Sheffield, J. and Milly, P.C. (2017) Divergent surface and total soil moisture projections under global warming. *Geophysical Research Letters*, 44(1), 236–244.

Blauhut, V., Gudmundsson, L. and Stahl, K. (2015) Towards pan-European drought risk maps: quantifying the link between drought indices and reported drought impacts. *Environmental Research Letters*, 10(1), 014008.

Boer, M.M., de Dios, V.R. and Bradstock, R.A. (2020) Unprecedented burn area of Australian mega forest fires. *Nature Climate Change*, 10(3), 171–172.

Burke, E.J. and Brown, S.J. (2008) Evaluating uncertainties in the projection of future drought. *Journal of Hydrometeorology*, 9(2), 292–299.

Calvin, K., Bond-Lamberty, B., Clarke, L., Edmonds, J., Eom, J., Hartin, C., Kim, S., Kyle, P., Link, R., Moss, R., McJeon, H., Patel, P., Smith, S., Waldhoff, S. and McJeon, H. (2017) The SSP4: a world of deepening inequality. *Global Environmental Change*, 42, 284–296.

Cammalleri, C., Micale, F. and Vogt, J. (2016) A novel soil moisture-based drought severity index (DSI) combining water deficit magnitude and frequency. *Hydrological Processes*, 30(2), 289–301.

Careto, J.A.M., Cardoso, R.M., Soares, P.M.M. and Trigo, R.M. (2018) Land-atmosphere coupling in CORDEX-Africa: Hindcast regional climate simulations. *Journal of Geophysical Research: Atmospheres*, 123(19), 11–48.

Carrao, H., Naumann, G. and Barbosa, P. (2016) Mapping global patterns of drought risk: an empirical framework based on sub-national estimates of hazard, exposure and vulnerability. *Global Environmental Change*, 39, 108–124.

Carrão, H., Naumann, G. and Barbosa, P. (2018) Global projections of drought hazard in a warming climate: a prime for disaster risk management. *Climate Dynamics*, 50(5–6), 2137–2155.

Charney, J., Stone, P.H. and Quirk, W.J. (1975) Drought in the Sahara: a biogeophysical feedback mechanism. *Science*, 187 (4175), 434–435.

Choat, B., Brodribb, T.J., Brodersen, C.R., Duursma, R.A., López, R. and Medlyn, B.E. (2018) Triggers of tree mortality under drought. *Nature*, 558(7711), 531–539.

Choat, B., Jansen, S., Brodribb, T.J., Cochard, H., Delzon, S., Bhaskar, R., Bucci, S.J., Feild, T.S., Gleason, S.M., Hacke, U.G., Jacobsen, A.L., Lens, F., Maherali, H., Martínez-Vilalta, J., Mayr, S., Mencuccini, M., Mitchell, P.J., Nardini, A., Pittermann, J., Pratt, R.B., Sperry, J.S., Westoby, M., Wright, I.J. and Zanne, A.E. (2012) Global convergence in the vulnerability of forests to drought. *Nature*, 491(7426), 752–755.

Cook, B.I., Anchukaitis, K.J., Touchan, R., Meko, D.M. and Cook, E.R. (2016) Spatiotemporal drought variability in the mediterranean over the last 900 years. *Journal of Geophysical Research*, 121, 2060–2074.

Cook, B.I., Ault, T.R. and Smerdon, J.E. (2015) Unprecedented 21st century drought risk in the American Southwest and Central Plains. *Science Advances*, 1(1), e1400082.

Cook, B.I., Mankin, J.S. and Anchukaitis, K.J. (2018) Climate change and drought: from past to future. *Current Climate Change Reports*, 4(2), 164–179.

Cook, B.I., Mankin, J.S., Marvel, K., Williams, A.P., Smerdon, J.E. and Anchukaitis, K.J. (2020) Twenty-first century drought projections in the CMIP6 forcing scenarios. *Earth's Future*, 8(6), e2019EF001461.

Cook, B.I., Smerdon, J.E., Seager, R. and Coats, S. (2014) Global warming and 21st century drying. *Climate Dynamics*, 43(9–10), 2607–2627.

Cullen, B.R., Johnson, I.R., Eckard, R.J., Lodge, G.M., Walker, R.G., Rawnsley, R.P. and McCaskill, M.R. (2009) Climate change effects on pasture systems in South-Eastern Australia. *Crop and Pasture Science*, 60(10), 933–942.

Dai, A. and Zhao, T. (2017) Uncertainties in historical changes and future projections of drought. Part I: estimates of historical drought changes. *Climatic Change*, 144(3), 519–533.

Diasso, U. and Abiodun, B.J. (2017) Drought modes in West Africa and how well CORDEX RCMs simulate them. *Theoretical and Applied Climatology*, 128(1–2), 223–240.

Ding, Y., Hayes, M.J. and Widhalm, M. (2011) Measuring economic impacts of drought: a review and discussion. *Disaster Prevention & Management*, 20(4), 434–446.

Doblas-Miranda, E., Alonso, R., Arnan, X., Bermejo, V., Brotons, L., de las Heras, J., Estiarte, M., Hódar, J.A., Llorens, P., Lloret, F., López-Serrano, F.R., Martínez-Vilalta, J., Moya, D., Peñuelas, J., Pino, J., Rodrigo, A., Roura-Pascual, N., Valladares, F., Vilà, M., Zamora, R. and Retana, J. (2017) A review of the combination among global change factors in forests, shrublands and pastures of the Mediterranean region: beyond drought effects. *Global and Planetary Change*, 148, 42–54.

Donohue, R.J., McVicar, T.R. and Roderick, M.L. (2010) Assessing the ability of potential evaporation formulations to capture the dynamics in evaporative demand within a changing climate. *Journal of Hydrology*, 386(1–4), 186–197.

Dosio, A. and Fischer, E.M. (2018) Will half a degree make a difference? Robust projections of indices of mean and extreme climate in Europe under 1.5°C, 2°C, and 3°C global warming. *Geophysical Research Letters*, 45(2), 935–944.

Dosio, A., Jones, R.G., Jack, C., Lennard, C., Nikulin, G. and Hewitson, B. (2019) What can we know about future precipitation in Africa? Robustness, significance and added value of projections from a large ensemble of regional climate models. *Climate Dynamics*, 53, 5833–5858.

Dosio, A., Mentaschi, L., Fischer, E.M. and Wyser, K. (2018) Extreme heat waves under 1.5°C and 2°C global warming. *Environmental Research Letters*, 13(5), 54006.

Driouech, F., Elrhaz, K., Moufouma, W., Khadija, O. and Saloua, A. (2020) Assessing future changes of climate extreme events in the CORDEX—MENA region using regional climate model ALADIN—climate. *Earth Systems and Environment*, 4, 477–492. https://doi.org/10.1007/s41748-020-00169-3.

Ebi, K.L. and Bowen, K. (2016) Extreme events as sources of health vulnerability: drought as an example. *Weather and Climate Extremes*, 11, 95–102.

Feyen, L., Ciscar, J.C., Gosling, S., Ibarreta, D. and Soria, A. (2020) *Climate Change Impacts and Adaptation in Europe. JRC PESETA IV Final Report*. Luxembourg: EUR 30180EN, Publications Office of the European Union. https://doi.org/10.2760/171121 JRC119178.

Ficklin, D.L., Abatzoglou, J.T., Robeson, S.M. and Dufficy, A. (2016) The influence of climate model biases on projections of aridity and drought. *Journal of Climate*, 29(4), 1269–1285.

Field, C.B., Barros, V., Stocker, T., Qin, D., Dokken, D.J., Ebi, K.L., Mastrandrea, M.D., Mach, K.J., Plattner, G.-K., Allen, S.K., Tignor, M. and Midgley, P.M. (Eds.). (2012) *IPCC, 2012: Managing the Risks of Extreme Events and Disasters to Advance Climate Change Adaptation. In: A Special Report of Working Groups I and II of the Intergovernmental Panel on Climate Change*, Vol. 30. Cambridge, UK, and New York, NY: Cambridge University Press, pp. 7575–7613.

Fricko, O., Havlik, P., Rogelj, J., Klimont, Z., Gusti, M., Johnson, N., Kolp, P., Strubegger, M., Valin, H., Amann, M., Ermolieva, T., Forsell, N., Herrero, M., Heyes, C., Kindermann, G., Krey, V., McCollum, D.L., Obersteiner, M., Pachauri, S., Rao, S., Schmid, E., Schoepp, W. and Riahi, K. (2017) The marker quantification of the shared socioeconomic pathway 2: a middle-of-the-road scenario for the 21st century. *Global Environmental Change*, 42, 251–267.

Friedlingstein, P., Meinshausen, M., Arora, V.K., Jones, C.D., Anav, A., Liddicoat, S.K. and Knutti, R. (2014) Uncertainties in CMIP5 climate projections due to carbon cycle feedbacks. *Journal of Climate*, 27(2), 511–526.

Fujimori, S., Hasegawa, T., Masui, T., Takahashi, K., Herran, D.S., Dai, H., Hijioka, Y. and Kainuma, M. (2017) SSP3: AIM implementation of shared socioeconomic pathways. *Global Environmental Change*, 42, 268–283.

Garreaud, R.D., Boisier, J.P., Rondanelli, R., Montecinos, A., Sepúlveda, H.H. and Veloso-Aguila, D. (2020) The Central Chile mega drought (2010–2018): a climate dynamics perspective. *International Journal of Climatology*, 40(1), 421–439.

Gidden, M.J., Riahi, K., Smith, S.J., Fujimori, S., Luderer, G., Kriegler, E., van Vuuren, D.P., van den Berg, M., Feng, L., Klein, D., Calvin, K., Doelman, J.C., Frank, S., Fricko, O.,

Harmsen, M., Hasegawa, T., Havlik, P., Hilaire, J., Hoesly, R., Horing, J., Popp, A., Stehfest, E., Takahashi, K., Giorgi, F. and Bi, X. (2019) Global emissions pathways under different socioeconomic scenarios for use in CMIP6: a dataset of harmonized emissions trajectories through the end of the century. *Geoscientific Model Development Discussions*, 12(4), 1443–1475.

Giorgi, F. and Bi, X. (2005) Regional changes in surface climate interannual variability for the 21st century from ensembles of global model simulations. *Geophysical Research Letters*, 32, L13701. https://doi.org/10.1029/2005GL023002.

Giorgi, F., Coppola, E. and Giuliani, G. (2017) Plans for RegCM4 CORDEX-CORE simulations. *EGUGA*, 19, EGU2017–2195.

Giorgi, F. and Gutowski, W.J., Jr. (2015) Regional dynamical downscaling and the CORDEX initiative. *Annual Review of Environment and Resources*, 40, 467–490.

Giorgi, F., Raffaele, F. and Coppola, E. (2019) The response of precipitation characteristics to global warming from climate projections. *Earth System Dynamics*, 10, 73–89.

Gornall, J., Betts, R., Burke, E., Clark, R., Camp, J., Willett, K. and Wiltshire, A. (2010) Implications of climate change for agricultural productivity in the early twenty-first century. *Philosophical Transactions of the Royal Society B: Biological Sciences*, 365 (1554), 2973–2989.

Gourdji, S.M., Sibley, A.M. and Lobell, D.B. (2013) Global crop exposure to critical high temperatures in the reproductive period: historical trends and future projections. *Environmental Research Letters*, 8(2), 024041.

Gray, C. and Mueller, V. (2012) Drought and population mobility in rural Ethiopia. *World Development*, 40(1), 134–145.

Greve, P., Orlowsky, B., Mueller, B., Sheffield, J., Reichstein, M. and Seneviratne, S.I. (2014) Global assessment of trends in wetting and drying over land. *Nature Geoscience*, 7(10), 716–721.

Griffin, D. and Anchukaitis, K.J. (2014) How unusual is the 2012–2014 California drought? *Geophysical Research Letters*, 41(24), 9017–9023.

Grossiord, C., Granier, A., Ratcliffe, S., Bouriaud, O., Bruelheide, H., Chećko, E., Forrester, D.I., Dawud, S.M., Finér, L., Pollastrini, M., Scherer-Lorenzen, M., Valladares, F., Bonal, D., Gessler, A., Grossiord, C., Granier, A., Ratcliffe, S., Bouriaud, O., Bruelheide, H. and Chećko, E. (2014) Tree diversity does not always improve resistance of forest ecosystems to drought. *Proceedings of the National Academy of Sciences*, 111(41), 14812–14815.

Gu, L., Chen, J., Yin, J., Sullivan, S.C., Hui-Min, W., Guo, S., Zhang, L. and Kim, J.-S. (2020) Projected increases in magnitude and socioeconomic exposure of global droughts in 1.5 and 2° C warmer climates. *Hydrology and Earth System Sciences*, 24 (1), 451–472.

Gutowski, W.L., Giorgi, F., Timbal, B., Frigon, A., Jacob, D., Kang, H.-S., Raghavan, K., Lee, B., Lennard, C., Nikulin, G., O'Rourke, E., Rixen, M., Solman, S., Stephenson, T. and Tangang, F. (2016) WCRP COordinated regional Downscaling EXperiment (CORDEX): a diagnostic MIP for CMIP6. *Geoscientific Model Development*, 9, 4087–4095.

Haines, A., Kovats, R.S., Campbell-Lendrum, D. and Corvalán, C. (2006) Climate change and human health: impacts, vulnerability and public health. *Public Health*, 120(7), 585–596.

Hansen, J., Ruedy, R., Sato, M. and Lo, K. (2010) Global surface temperature change. *Reviews of Geophysics*, 48(4), RG4004.

Hao, Z. and Singh, V.P. (2015) Drought characterization from a multivariate perspective: a review. *Journal of Hydrology*, 527, 668–678.

Hare, B., Roming, N., Schaeffer, M. and Schleussner, C.-F. (2016) *Implications of the 1.5°C Limit in the Paris Agreement for Climate Policy and Decarbonisation*. Berlin: Climate Analytics, p. 25.

Hargreaves, G.H. and Samani, Z.A. (1985) Reference crop evapotranspiration from temperature. *Applied Engineering in Agriculture*, 1(2), 96–99.

Harris, I., Osborn, T.J., Jones, P. and Lister, D. (2020) Version 4 of the CRU TS monthly high-resolution gridded multivariate climate dataset. *Scientific Data*, 7(1), 1–18.

Hawkins, E., Ortega, P., Suckling, E., Schurer, A., Hegerl, G., Jones, P., Joshi, M., Osborn, T.J., Masson-Delmotte, V., Mignot, J., Thorne, P. and Jan van Oldenborgh, G. (2017) Estimating changes in global temperature since the preindustrial period. *Bulletin of the American Meteorological Society*, 98(9), 1841–1856.

Heim, R.R., Jr. (2002) A review of twentieth-century drought indices used in the United States. *Bulletin of the American Meteorological Society*, 83(8), 1149–1166.

Hirvonen, K., Sohnesen, T.P. and Bundervoet, T. (2020) Impact of Ethiopia's 2015 drought on child undernutrition. *World Development*, 131, 104964.

Hlásny, T., Mátyás, C., Seidl, R., Kulla, L., Merganičová, K., Trombik, J., Dobor, L., Barcza, Z. and Konôpka, B. (2014) Climate change increases the drought risk in central European forests: what are the options for adaptation? *Central European Forestry Journal*, 60(1), 5–18.

Howitt, R., Medellín-Azuara, J., MacEwan, D., Lund, J.R. and Sumner, D. (2014) Economic Analysis of the 2014 Drought for California Agriculture. University of California, Davis, CA: *Center for Watershed Sciences.*

Hurtt, G.C., Chini, L.P., Sahajpal, R., Frolking, S.E., Bodirsky, B., Calvin, K.V., Doelman, J.C., Fisk, J., Fujimori, S., Goldewijk, K. & Hasegawa, T., Havlik, P., Heinimann, A., Humpenöder, F., Jungclaus, J., Kaplan, J.O., Krisztin, T., Lawrence, D. M., Lawrence, P., Mertz, O., Pongratz, J., Popp, A., Poulter, B., Riahi, K., Shevliakova, E., Stehfest, E., Thornton, P. E., van Vuuren, D. and Zhang, X. (2018) LUH2: harmonization of global land-use scenarios for the period 850-2100. *AGUFM, 2018*, GC13A-01.

Iglesias, A., Garrote, L., Flores, F. and Moneo, M. (2007) Challenges to manage the risk of water scarcity and climate change in the Mediterranean. *Water Resources Management*, 21(5), 775–788.

IPCC. (2018) 2018: Global warming of 1.5°C. an IPCC special report on the impacts of global warming of 1.5°C above pre-industrial levels and related global greenhouse gas emission pathways. In: Masson-Delmotte, V., Zhai, P., Pörtner, H.O., Roberts, D., Skea, J., Shukla, P.R., Pirani, A., Moufouma-Okia, W., Péan, C., Pidcock, R., Connors, S., Matthews, J.B.R., Chen, Y., Zhou, X., Gomis, M.I., Lonnoy, E., Maycock, T., Tignor, M. and Waterfield, T. (Eds.) *The Context of Strengthening the Global Response to the Threat of Climate Change, Sustainable Development, and Efforts to Eradicate Poverty*. Geneva, Switzerland: World Meteorological Organization.

Iturbide, M., Gutiérrez, J.M., Alves, L.M., Bedia, J., Cimadevilla, E., Cofiño, A.S., Di Luca, A., Faria, S.H., Gorodetskaya, I.V. and

Hauser, M. (2020) An update of IPCC climate reference regions for subcontinental analysis of climate model data: definition and aggregated datasets. *Earth System Science Data Discussions*, 12, 2959–2970.

Jacob, D., Petersen, J., Eggert, B., Alias, A., Christensen, O.B., Bouwer, L.M., Braun, A., Colette, A., Déqué, M., Georgievski, G., Georgopoulou, E., Gobiet, A., Menut, L., Nikulin, G., Haensler, A., Hempelmann, N., Jones, C., Keuler, K., Kovats, S., Kröner, N., Kotlarski, S., Kriegsmann, A., Martin, E., van Meijgaard, E., Moseley, C., Pfeifer, S., Preuschmann, S., Radermacher, C., Radtke, K., Rechid, D., Rounsevell, M., Samuelsson, P., Somot, S., Soussana, J.-F., Teichmann, C., Valentini, R., Vautard, R., Weber, B. and Yiou, P. (2014) EURO-CORDEX: new high-resolution climate change projections for European impact research. *Regional Environmental Change*, 14(2), 563–578.

Jeong, D.I., Sushama, L. and Khaliq, M.N. (2014) The role of temperature in drought projections over North America. *Climatic Change*, 127(2), 289–303.

Jones, B. and O'Neill, B.C. (2016) Spatially explicit global population scenarios consistent with the shared socioeconomic pathways. *Environmental Research Letters*, 11(8), 084003.

Jones, B. and O'Neill, B.C. (2020) *Global One-Eighth Degree Population Base Year and Projection Grids Based on the Shared Socioeconomic Pathways, Revision 01*. Palisades, NY: NASA Socioeconomic Data and Applications Center (SEDAC). https://doi.org/10.7927/m30p-j498 [Accessed 12th May 2020].

Kamali, B., Abbaspour, K.C., Lehmann, A., Wehrli, B. and Yang, H. (2018) Spatial assessment of maize physical drought vulnerability in sub-Saharan Africa: linking drought exposure with crop failure. *Environmental Research Letters*, 13(7), 074010.

Keeling, H.C. and Phillips, O.L. (2007) The global relationship between forest productivity and biomass. *Global Ecology and Biogeography*, 16(5), 618–631.

Kiem, A.S., Johnson, F., Westra, S., van Dijk, A., Evans, J.P., O'Donnell, A., Rouillard, A., Barr, C., Tyler, J., Thyer, M., Jakob, D., Woldemeskel, F., Sivakumar, B. and Mehrotra, R. (2016) Natural hazards in Australia: droughts. *Climatic Change*, 139(1), 37–54.

Kim, H., Park, J., Yoo, J. and Kim, T.W. (2015) Assessment of drought hazard, vulnerability, and risk: a case study for administrative districts in South Korea. *Journal of Hydro-Environment Research*, 9(1), 28–35.

Kjellström, E., Nikulin, G., Strandberg, G., Christensen, O.B., Jacob, D., Keuler, K., Lenderink, G., van Meijgaard, E., Schär, C., Somot, S., Sørland, S.L., Teichmann, C. and Vautard, R. (2018) European climate change at global mean temperature increases of 1.5 and 2 degrees C above pre-industrial conditions as simulated by the EURO-CORDEX regional climate models. *Earth System Dynamics*, 9(2), 459–478.

Knox, J., Hess, T., Daccache, A. and Wheeler, T. (2012) Climate change impacts on crop productivity in Africa and South Asia. *Environmental Research Letters*, 7(3), 034032.

Knutti, R. and Sedláček, J. (2013) Robustness and uncertainties in the new CMIP5 climate model projections. *Nature Climate Change*, 3(4), 369–373.

Kriegler, E., Bauer, N., Popp, A., Humpenöder, F., Leimbach, M., Strefler, J., Baumstark, L., Bodirsky, B.L., Hilaire, J., Klein, D., Mouratiadou, I., Weindl, I., Bertram, C., Dietrich, J.-P., Luderer, G., Pehl, M., Pietzcker, R., Piontek, F., Lotze-Campen, H., Biewald, A., Bonsch, M., Giannousakis, A., Kreidenweis, U., Müller, C., Rolinski, S., Schultes, A., Schwanitz, J., Stevanovic, M., Calvin, K., Emmerling, J., Fujimori, S. and Edenhofer, O. (2017) Fossil-fueled development (SSP5): an energy and resource intensive scenario for the 21st century. *Global Environmental Change*, 42, 297–315.

Kumar, S., Molitor, R. and Vollmer, S. (2016) Drought and early child health in rural India. *Population and Development Review*, 42, 53–68.

Kurz, W.A., Dymond, C.C., Stinson, G., Rampley, G.J., Neilson, E. T., Carroll, A.L., Ebata, T. and Safranyik, L. (2008) Mountain pine beetle and forest carbon feedback to climate change. *Nature*, 452(7190), 987–990.

Legasa, M.N., Manzanas, R., Fernández, J., Herrera, S., Iturbide, M., Moufouma-Okia, W., Zhai, P., Driouech, F. and Gutiérrez, J.M. (2020) Assessing multidomain overlaps and grand ensemble generation in CORDEX regional projections. *Geophysical Research Letters*, 47(4), e2019GL086799.

Lehner, F., Coats, S., Stocker, T.F., Pendergrass, A.G., Sanderson, B. M., Raible, C.C. and Smerdon, J.E. (2017) Projected drought risk in 1.5 C and 2 C warmer climates. *Geophysical Research Letters*, 44(14), 7419–7428.

Leimbach, M., Kriegler, E., Roming, N. and Schwanitz, J. (2017) Future growth patterns of world regions–a GDP scenario approach. *Global Environmental Change*, 42, 215–225.

Leng, G. and Hall, J. (2019) Crop yield sensitivity of global major agricultural countries to droughts and the projected changes in the future. *Science of the Total Environment*, 654, 811–821.

Lesk, C., Rowhani, P. and Ramankutty, N. (2016) Influence of extreme weather disasters on global crop production. *Nature*, 529(7584), 84–87.

Li, Y., Ye, W., Wang, M. and Yan, X. (2009) Climate change and drought: a risk assessment of crop-yield impacts. *Climate Research*, 39(1), 31–46.

Liu, W., Sun, F., Lim, W.H., Zhang, J., Wang, H., Shiogama, H. and Zhang, Y. (2018) Global drought and severe drought-affected populations in 1.5 and 2 °C warmer worlds. *Earth System Dynamics*, 9(1), 267–283.

Lloyd-Hughes, B. (2014) The impracticality of a universal drought definition. *Theoretical and Applied Climatology*, 117(3–4), 607–611.

Loboda, T., Krankina, O., Savin, I., Kurbanov, E. and Hall, J. (2017) Land management and the impact of the 2010 extreme drought event on the agricultural and ecological systems of European Russia. In: *Land-Cover and Land-Use Changes in Eastern Europe after the Collapse of the Soviet Union in 1991*. Cham: Springer, pp. 173–192.

Logar, I. and van den Bergh, J.C. (2013) Methods to assess costs of drought damages and policies for drought mitigation and adaptation: review and recommendations. *Water Resources Management*, 27(6), 1707–1720.

Marengo, J.A., Torres, R.R. and Alves, L.M. (2017) Drought in northeast Brazi—past, present, and future. *Theoretical and Applied Climatology*, 129(3–4), 1189–1200.

Marx, A., Kumar, R., Thober, S., Rakovec, O., Wanders, N., Zink, M., Wood, E.F., Pan, M., Sheffield, J. and Samaniego, L. (2018) Climate change alters low flows in Europe under global warming of 1.5, 2, and 3 C. *Hydrology and Earth System Sciences*, 22(2), 1017–1032.

McDowell, N.G. and Allen, C.D. (2015) Darcy's law predicts widespread forest mortality under climate warming. *Nature Climate Change*, 5(7), 669–672.

McDowell, N.G., Allen, C.D., Anderson-Teixeira, K., Aukema, B.H., Bond-Lamberty, B., Chini, L., Clark, J.S., Dietze, M., Grossiord, C., Hanbury-Brown, A., Hurtt, G.C., Jackson, R.B., Johnson, D. J., Kueppers, L., Lichstein, J.W., Ogle, K., Poulter, B., Pugh, T.A. M., Seidl, R., Turner, M.G., Uriarte, M., Walker, A.P. and Xu, C. (2020) Pervasive shifts in forest dynamics in a changing world. *Science*, 368(6494), eaaz9463.

McKee, T.B., Doesken, N.J. and Kleist, J. (1993, January) The relationship of drought frequency and duration to time scales. In: *Proceedings of the 8th Conference on Applied Climatology*, Vol. 17, No. 22. Anaheim, California: Eighth Conference on Applied Climatology, pp. 179–183.

Medellín-Azuara, J., MacEwan, D., Howitt, R.E., Sumner, D.A., Lund, J.R., Scheer, J., Gailey, R., Hart, Q., Alexander, N.D., Arnold, B., Kwon, A., Bell, A. and Li, W. (2016) Economic analysis of the 2016 California drought on agriculture. In: *Center for Watershed Sciences*. Davis, CA: UC Davis.

Meza, I., Siebert, S., Döll, P., Kusche, J., Herbert, C., Eyshi Rezaei, E., Nouri, H., Gerdener, H., Popat, E., Frischen, J., Naumann, G., Vogt, J.V., Walz, Y., Sebesvari, Z. and Hagenlocher, M. (2020) Global-scale drought risk assessment for agricultural systems. *Natural Hazards and Earth System Sciences*, 20, 695–712. https://doi.org/10.5194/nhess-20-695-2020.

Mishra, A.K. and Singh, V.P. (2010) A review of drought concepts. *Journal of Hydrology*, 391(1–2), 202–216.

Mishra, A.K. and Singh, V.P. (2011) Drought modeling–a review. *Journal of Hydrology*, 403(1–2), 157–175.

Miyan, M.A. (2015) Droughts in Asian least developed countries: vulnerability and sustainability. *Weather and Climate Extremes*, 7, 8–23.

Nam, W.H., Hayes, M.J., Svoboda, M.D., Tadesse, T. and Wilhite, D.A. (2015) Drought hazard assessment in the context of climate change for South Korea. *Agricultural Water Management*, 160, 106–117.

O'Brien, L.V., Berry, H.L., Coleman, C. and Hanigan, I.C. (2014) Drought as a mental health exposure. *Environmental Research*, 131, 181–187.

O'Neill, B.C., Kriegler, E., Ebi, K.L., Kemp-Benedict, E., Riahi, K., Rothman, D.S., van Ruijven, B.J., van Vuuren, D.P., Birkmann, J., Kok, K., Levy, M. and Solecki, W. (2017) The roads ahead: narratives for shared socioeconomic pathways describing world futures in the 21st century. *Global Environmental Change*, 42, 169–180.

O'Neill, B.C., Kriegler, E., Riahi, K., Ebi, K.L., Hallegatte, S., Carter, T.R., Mathur, R. and van Vuuren, D.P. (2014) A new scenario framework for climate change research: the concept of shared socioeconomic pathways. *Climatic Change*, 122(3), 387–400.

O'Neill, B.C., Tebaldi, C., van Vuuren, D.P., Eyring, V., Friedlingstein, P., Hurtt, G., Knutti, R., Kriegler, E., Lamarque, J.-F., Lowe, J., Meehl, G.A., Moss, R., Riahi, K. and Sanderson, B.M. (2016) The scenario model Intercomparison project (ScenarioMIP) for CMIP6. *Geoscientific Model Development*, 9 (9), 3461–3482.

Orlowsky, B. and Seneviratne, S.I. (2013) Elusive drought: uncertainty in observed trends and short-andlong-term CMIP5 projections. *Hydrology and Earth System Sciences*, 17(5), 1765–1781.

Otto, F.E., Wolski, P., Lehner, F., Tebaldi, C., Van Oldenborgh, G. J., Hogesteeger, S., Singh, R., Holden, P., Fučkar, N.S., Odoulami, R.C. and New, M. (2018) Anthropogenic influence on the drivers of the Western cape drought 2015–2017. *Environmental Research Letters*, 13(12), 124010.

IPCC. (2014) Climate change 2014: synthesis report. In: Pachauri, R.K. and Meyer, L.A. (Eds.) *Contribution of Working Groups I, II and III to the Fifth Assessment Report of the Intergovernmental Panel on Climate Change*. Geneva, Switzerland: IPCC, p. 151.

Parry, M.A.J., Flexas, J. and Medrano, H. (2005) Prospects for crop production under drought: research priorities and future directions. *Annals of Applied Biology*, 147(3), 211–226.

Pattnayak, K.C., Panda, S.K., Saraswat, V. and Dash, S.K. (2018) Assessment of two versions of regional climate model in simulating the Indian summer monsoon over South Asia CORDEX domain. *Climate Dynamics*, 50(7–8), 3049–3061.

Peduzzi, P., Dao, H., Herold, C. and Mouton, F. (2009) Assessing global exposure and vulnerability towards natural hazards: the disaster risk index. *Natural Hazards and Earth System Sciences*, 9(4), 1149–1159.

Penalba, O.C. and Rivera, J.A. (2013) Future changes in drought characteristics over southern South America projected by a CMIP5 multi-model ensemble. *American Journal of Climate Change*, 2, 173–182.

Perera, R.S., Cullen, B.R. and Eckard, R.J. (2019) Growth and physiological responses of temperate pasture species to consecutive heat and drought stresses. *Plants*, 8(7), 227.

Pomeroy, J.W., Gray, D.M., Brown, T., Hedstrom, N.R., Quinton, W.L., Granger, R.J. and Carey, S.K. (2007) The cold regions hydrological model: a platform for basing process representation and model structure on physical evidence. *Hydrological Processes: An International Journal*, 21(19), 2650–2667.

Prestele, R., Alexander, P., Rounsevell, M.D., Arneth, A., Calvin, K., Doelman, J., Eitelberg, D.A., Engström, K., Fujimori, S., Hasegawa, T., Havlik, P., Humpenöder, F., Jain, A.K., Krisztin, T., Kyle, P., Meiyappan, P., Popp, A., Sands, R.D., Schaldach, R., Schüngel, J., Stehfest, E., Tabeau, A., Meijl, H.V., Vliet, J.V. and Verburg, P.H. (2016) Hotspots of uncertainty in land-use and land-cover change projections: a global-scale model comparison. *Global Change Biology*, 22(12), 3967–3983.

Rebetez, M., Mayer, H., Dupont, O., Schindler, D., Gartner, K., Kropp, J.P. and Menzel, A. (2006) Heat and drought 2003 in Europe: a climate synthesis. *Annals of Forest Science*, 63(6), 569–577.

Reed, M.S. and Stringer, L.C. (2016) *Land Degradation, Desertification and Climate Change: Anticipating, Assessing and Adapting to Future Change*. New York: Routledge.

Rennenberg, H., Loreto, F., Polle, A., Brilli, F., Fares, S., Beniwal, R.S. and Gessler, A. (2006) Physiological responses of forest trees to heat and drought. *Plant Biology*, 8(05), 556–571.

Riahi, K., Rao, S., Krey, V., Cho, C., Chirkov, V., Fischer, G., Kindermann, G., Nakicenovic, N. and Rafaj, P. (2011) RCP 8.5—a scenario of comparatively high greenhouse gas emissions. *Climatic Change*, 109(1–2), 33–57.

Riahi, K., Van Vuuren, D.P., Kriegler, E., Edmonds, J., O'Neill, B. C., Fujimori, S., Bauer, N., Calvin, K., Dellink, R., Fricko, O., Lutz, W., Popp, A., Cuaresma, J.C., Samir, K.C., Leimbach, M.,

Jiang, L., Kram, T., Rao, S., Emmerling, J., Ebi, K., Hasegawa, T., Havlik, P., Humpenöder, F., Da Silva, L.A., Smith, S., Stehfest, E., Bosetti, V., Eom, J., Gernaat, D., Masui, T., Rogelj, J., Strefler, J., Drouet, L., Krey, V., Luderer, G., Harmsen, M., Takahashi, K., Baumstark, L., Doelman, J.C., Kainuma, M., Klimont, Z., Marangoni, G., Lotze-Campen, H., Obersteiner, M., Tabeau, A. and Tavoni, M. (2017) The shared socioeconomic pathways and their energy, land use, and greenhouse gas emissions implications: an overview. *Global Environmental Change*, 42, 153–168.

Rogelj, J., Meinshausen, M. and Knutti, R. (2012) Global warming under old and new scenarios using IPCC climate sensitivity range estimates. *Nature Climate Change*, 2(4), 248–253.

Rolo, V. and Moreno, G. (2019) Shrub encroachment and climate change increase the exposure to drought of Mediterranean wood-pastures. *Science of the Total Environment*, 660, 550–558.

Samaniego, L., Kumar, R., Breuer, L., Chamorro, A., Flörke, M., Pechlivanidis, I.G., Schäfer, D., Shah, H., Vetter, T., Wortmann, M. and Zeng, X. (2017) Propagation of forcing and model uncertainties into hydrological drought characteristics in a multi-model century-long experiment in large river basins. *Climatic Change*, 141(3), 435–449.

Samaniego, L., Thober, S., Kumar, R., Wanders, N., Rakovec, O., Pan, M., Zink, M., Sheffield, J., Wood, E.F. and Marx, A. (2018) Anthropogenic warming exacerbates European soil moisture droughts. *Nature Climate Change*, 8(5), 421–426.

Samantaray, A.K., Ramadas, M. and Panda, R.K. (2021) Assessment of impacts of potential climate change on meteorological drought characteristics at regional scales. *International Journal of Climatology.*, 41(Suppl. 1), E319–E341. https://doi.org/10.1002/joc.6687.

Samir, K.C. and Lutz, W. (2014) Demographic scenarios by age, sex and education corresponding to the SSP narratives. *Population and Environment*, 35(3), 243–260.

Schneider, U., Becker, A., Finger, P., Meyer-Christoffer, A., Rudolf, B. and Ziese, M. (2011) GPCC full data reanalysis version 6.0 at 0.5: monthly land-surface precipitation from rain-gauges built on GTS-based and historic data. *GPCC Data Rep*. doi: https://doi.org/10.5676/DWD_GPCC/FD_M_V6_050.

Schneider, U., Becker, A., Finger, P., Meyer-Christoffer, A. and Ziese, M. (2018) GPCC full data monthly version 2018 at 0.5°: monthly land-surface precipitation from rain-gauges built on GTS-based and historical data. *Global Precipitation Climatology Centre (GPCC) at Deutscher Wetterdienst*. doi:https://doi.org/10.5676/DWD_GPCC/FD_M_V2018_050

Schwalm, C.R., Anderegg, W.R., Michalak, A.M., Fisher, J.B., Biondi, F., Koch, G., Litvak, M., Ogle, K., Shaw, J.D., Wolf, A., Huntzinger, D.N., Schaefer, K., Cook, R., Wei, Y., Fang, Y., Hayes, D., Huang, M., Jain, A. and Tian, H. (2017) Global patterns of drought recovery. *Nature*, 548(7666), 202–205.

Schwalm, C.R., Williams, C.A., Schaefer, K., Baldocchi, D., Black, T.A., Goldstein, A.H., Law, B.E., Oechel, W.C., Paw U, K.T. and Scott, R.L. (2012) Reduction in carbon uptake during turn of the century drought in western North America. *Nature Geoscience*, 5(8), 551–556.

Seager, R., Hoerling, M., Schubert, S., Wang, H., Lyon, B., Kumar, A., Nakamura, J. and Henderson, N. (2015) Causes of the 2011–14 California drought. *Journal of Climate*, 28(18), 6997–7024.

Seidl, R., Thom, D., Kautz, M., Martin-Benito, D., Peltoniemi, M., Vacchiano, G., Wild, J., Ascoli, D., Petr, M., Honkaniemi, J., Lexer, M.J., Trotsiuk, V., Mairota, P., Svoboda, M., Fabrika, M., Nagel, T.A. and Reyer, C.P.O. (2017) Forest disturbances under climate change. *Nature Climate Change*, 7(6), 395–402.

Seneviratne, S.I. (2012) Climate science: historical drought trends revisited. *Nature*, 491(7424), 338–339.

Sheffield, J. and Wood, E.F. (2008) Global trends and variability in soil moisture and drought characteristics, 1950–2000, from observation-driven simulations of the terrestrial hydrologic cycle. *Journal of Climate*, 21(3), 432–458.

Sheffield, J. and Wood, E.F. (2011) *Drought: Past Problems and Future Scenarios*. London and Washington, DC: Earthscan, p. 211.

Sheffield, J., Wood, E.F. and Roderick, M.L. (2012) Little change in global drought over the past 60 years. *Nature*, 491(7424), 435–438.

Smirnov, O., Zhang, M., Xiao, T., Orbell, J., Lobben, A. and Gordon, J. (2016) The relative importance of climate change and population growth for exposure to future extreme droughts. *Climatic Change*, 138(1–2), 41–53.

Soussana, J.F., Graux, A.I. and Tubiello, F.N. (2010) Improving the use of modelling for projections of climate change impacts on crops and pastures. *Journal of Experimental Botany*, 61(8), 2217–2228.

Spinoni, J., Barbosa, P., Bucchignani, E., Cassano, J., Cavazos, T., Christensen, J.H., Christensen, O.B., Coppola, E., Evans, J., Geyer, B., Giorgi, F., Hadjinicolaou, P., Jacob, D., Katzfey, J., Koenigk, T., Laprise, R., Lennard, C.J., Levent Kurnaz, M., Li, D., Llopart, M., McCormick, N., Naumann, G., Nikulin, G., Ozturk, T., Panitz, H.-J., da Rocha, R.P., Rockel, B., Solman, S. A., Syktus, J., Tangang, F., Teichmann, C., Vautard, R., Vogt, J. V., Winger, K., Zittis, G. and Dosio, A. (2020) Future global meteorological drought hotspots: a study based on CORDEX data. *Journal of Climate*, 33(9), 3635–36561.

Spinoni, J., Barbosa, P., De Jager, A., McCormick, N., Naumann, G., Vogt, J.V., Magni, D., Masante, D. and Mazzeschi, M. (2019) A new global database of meteorological drought events from 1951 to 2016. *Journal of Hydrology: Regional Studies*, 22, 100593.

Spinoni, J., Naumann, G., Carrao, H., Barbosa, P. and Vogt, J. (2014) World drought frequency, duration, and severity for 1951–2010. *International Journal of Climatology*, 34(8), 2792–2804.

Spinoni, J., Naumann, G. and Vogt, J.V. (2017) Pan-European seasonal trends and recent changes of drought frequency and severity. *Global and Planetary Change*, 148, 113–130.

Spinoni, J., Vogt, J.V., Naumann, G., Barbosa, P. and Dosio, A. (2018) Will drought events become more frequent and severe in Europe? *International Journal of Climatology*, 38(4), 1718–1736.

Steffen, W., Richardson, K., Rockström, J., Cornell, S.E., Fetzer, I., Bennett, E.M., Biggs, R., Carpenter, S.R., de Vries, W., de Wit, C.A., Folke, C., Gerten, D., Heinke, J., Mace, G.M., Persson, L. M., Ramanathan, V., Reyers, B. and Sörlin, S. (2015) Planetary boundaries: guiding human development on a changing planet. *Science*, 347(6223), 1259855.

Su, B., Huang, J., Fischer, T., Wang, Y., Kundzewicz, Z.W., Zhai, J., Sun, H., Wang, A., Zeng, X., Wang, G., Tao, H., Gemmer, M., Li, X. and Jiang, T. (2018) Drought losses in China might

double between the 1.5C and 2.0C warming. *Proceedings of the National Academy of Sciences*, 115(42), 10600–10605.

Supari, S., Tangang, F., Juneng, L., Cruz, F., Chung, J.X., Ngai, S.T., Salimun, E., Mohd, M.S.F., Santisirisomboon, J., Singhruck, P., Phan-Van, T., Ngo-Duc, T., Narisma, G., Aldrian, E., Gunawan, D. and Supaheluwakan, A. (2020) Multi-model projections of precipitation extremes in Southeast Asia based on CORDEX-Southeast Asia simulations. *Environmental Research*, 184, 109350.

Swain, S. and Hayhoe, K. (2015) CMIP5 projected changes in spring and summer drought and wet conditions over North America. *Climate Dynamics*, 44(9–10), 2737–2750.

Tamoffo, X., Dosio, A., Vondou, D.A. and Sonkoué, D. (2020) Process-based analysis of the added value of dynamical downscaling over Central Africa. *Geophysical Research Letters*, 47, e2020GL089702. https://doi.org/10.1029/2020GL089702.

Tangang, F., Chung, J.X., Juneng, L., Supari, Salimun, E., Ngai, S. T., Jamaluddin, A.F., Faisal, M.S., Cruz, F., Narisma, G.T., Santisirisomboon, J., Ngo-Duc, T., Phan, V.T., Singhruck, P., Gunawan, D., Aldrian, E., Sopaheluwakan, A., Nikulin, G., Remedio, A.R.C., Sein, D.V., Hein-Griggs, D. and Mcgregor, J. L. (2020) Projected future changes in rainfall in Southeast Asia based on CORDEX—SEA multi-model simulations. *Climate Dynamics*, 55, 1247–1267.

Taylor, I.H., Burke, E., McColl, L., Falloon, P.D., Harris, G.R. and McNeall, D. (2013) The impact of climate mitigation on projections of future drought. *Hydrology and Earth System Sciences*, 17(6), 2339–2358.

Thomson, A.M., Calvin, K.V., Smith, S.J., Kyle, G.P., Volke, A., Patel, P., Delgado-Arias, S., Bond-Lamberty, B., Wise, M.A., Clarke, L.E. and Edmonds, J.A. (2011) RCP4. 5: a pathway for stabilization of radiative forcing by 2100. *Climatic Change*, 109 (1–2), 77–94.

Toreti, A., Cronie, O. and Zampieri, M. (2019) Concurrent climate extremes in the key wheat producing regions of the world. *Scientific Reports*, 9(1), 1–8.

Trenberth, K.E., Dai, A., Van Der Schrier, G., Jones, P.D., Barichivich, J., Briffa, K.R. and Sheffield, J. (2014) Global warming and changes in drought. *Nature Climate Change*, 4(1), 17–22.

Tubiello, F.N., Soussana, J.F. and Howden, S.M. (2007) Crop and pasture response to climate change. *Proceedings of the National Academy of Sciences*, 104(50), 19686–19690.

Ukkola, A.M., De Kauwe, M.G., Roderick, M.L., Abramowitz, G. and Pitman, A.J. (2020) Robust future changes in meteorological drought in CMIP6 projections despite uncertainty in precipitation. *Geophysical Research Letters*, 47(11), e2020GL087820.

UNFCCC, 2015. Paris agreement to the United Nations framework convention on climate change, Dec. 12, 2015, T.I.a.S. no. 16-1104.

Van Dijk, A.I., Beck, H.E., Crosbie, R.S., de Jeu, R.A., Liu, Y.Y., Podger, G.M., Timbal, B. and Viney, N.R. (2013) The millennium drought in Southeast Australia (2001–2009): natural and human causes and implications for water resources, ecosystems, economy, and society. *Water Resources Research*, 49(2), 1040–1057.

Van Vuuren, D.P. and Carter, T.R. (2014) Climate and socio-economic scenarios for climate change research and assessment: reconciling the new with the old. *Climatic Change*, 122(3), 415–429.

Van Vuuren, D.P., Edmonds, J.A., Kainuma, M., Riahi, K. and Weyant, J. (2011a) A special issue on the RCPs. *Climatic Change*, 109(1–2), 1–4.

Van Vuuren, D.P., Stehfest, E., den Elzen, M.G., Kram, T., van Vliet, J., Deetman, S., Isaac, M., Goldewijk, K.K., Hof, A., Beltran, A.M., Oostenrijk, R. and van Ruijven, B. (2011b) RCP2.6: exploring the possibility to keep global mean temperature increase below 2°C. *Climatic Change*, 109(1–2), 95–116.

Van Vuuren, D.P., Stehfest, E., Gernaat, D.E., Doelman, J.C., Van den Berg, M., Harmsen, M., de Boer, H.S., Bouwman, L.F., Daioglou, V., Edelenbosch, O.Y., Girod, B., Kram, T., Lassaletta, L., Lucas, P.L., van Meijl, H., Müller, C., van Ruijven, B.J., van der Sluis, S. and Tabeau, A. (2017) Energy, land-use and greenhouse gas emissions trajectories under a green growth paradigm. *Global Environmental Change*, 42, 237–250.

Vautard, R., Gobiet, A., Sobolowski, S., Kjellström, E., Stegehuis, A., Watkiss, P., Mendlik, T., Landgren, O., Nikulin, G., Teichmann, C. and Jacob, D. (2014) The European climate under a 2 °C global warming. *Environmental Research Letters*, 9 (3), 034006.

Vicente-Serrano, S.M., Beguería, S. and López-Moreno, J.I. (2010) A multiscalar drought index sensitive to global warming: the standardized precipitation evapotranspiration index. *Journal of Climate*, 23(7), 1696–1718.

Vicente-Serrano, S.M., Gouveia, C., Camarero, J.J., Beguería, S., Trigo, R., López-Moreno, J.I., Azorín-Molina, C., Pasho, E., Lorenzo-Lacruz, J., Revuelto, J., Morán-Tejeda, E. and Sanchez-Lorenzo, A. (2013) Response of vegetation to drought time-scales across global land biomes. *Proceedings of the National Academy of Sciences*, 110(1), 52–57.

Vogt, J.V. and Somma, F. (2000) *Drought and Drought Mitigation in Europe*, Vol. 14. Berlin/Heidelberg, Germany: Springer Science & Business Media.

Wegren, S.K. (2011) Food security and Russia's 2010 drought. *Eurasian Geography and Economics*, 52(1), 140–156.

Wehner, M., Easterling, D.R., Lawrimore, J.H., Heim, R.R., Jr., Vose, R.S. and Santer, B.D. (2011) Projections of future drought in the continental United States and Mexico. *Journal of Hydrometeorology*, 12(6), 1359–1377.

Weiss, M. and Menzel, L. (2008) A global comparison of four potential evapotranspiration equations and their relevance to stream flow modelling in semi-arid environments. *Advances in Geosciences*, 18, 15–23.

Wilhite, D., Easterling, W., Wood, D.A. and Rasmusson, E. (2019) *Planning for Drought: Toward a Reduction of Societal Vulnerability*. Taylor and Francis, New York, US: Routledge.

Wilhite, D.A. (1993) Planning for drought: a methodology. In: *Drought Assessment, Management, and Planning: Theory and Case Studies*. Boston, MA: Springer, pp. 87–108.

Wilhite, D.A. (2000) Drought as a natural hazard: concepts and definitions. In: Wilhite, D.A. (Ed.) *Drought: A Global Assessment*, Vol. 1. New York: Routledge, pp. 1–18.

Wilhite, D.A. and Buchanan-Smith, M. (2005) Drought as hazard: understanding the natural and social context. *Drought and water crises: Science, technology, and management issues*. Boca Raton: CRC Press, pp. 3–29.

Wilhite, D.A., Sivakumar, M.V. and Pulwarty, R. (2014) Managing drought risk in a changing climate: the role of national drought policy. *Weather and Climate Extremes*, 3, 4–13.

Wilhite, D.A., Svoboda, M.D. and Hayes, M.J. (2007) Understanding the complex impacts of drought: a key to enhancing drought mitigation and preparedness. *Water Resources Management*, 21 (5), 763–774.

Williams, A.P., Allen, C.D., Macalady, A.K., Griffin, D., Woodhouse, C.A., Meko, D.M., Swetnam, T.W., Rauscher, S.A., Seager, R., Grissino-Mayer, H.D., Dean, J.S., Cook, E.R., Gangodagamage, C., Cai, M. and McDowell, N.G. (2013) Temperature as a potent driver of regional forest drought stress and tree mortality. *Nature Climate Change*, 3(3), 292–297.

Williams, A.P., Seager, R., Abatzoglou, J.T., Cook, B.I., Smerdon, J. E. and Cook, E.R. (2015) Contribution of anthropogenic warming to California drought during 2012–2014. *Geophysical Research Letters*, 42(16), 6819–6828.

Winsemius, H.C., Jongman, B., Veldkamp, T.I., Hallegatte, S., Bangalore, M. and Ward, P.J. (2015) Disaster risk, climate change, and poverty: assessing the global exposure of poor people to floods and droughts. *Environment and Development Economics*, 23(3), 328–348.

Wyser, K., Kjellström, E., Koenigk, T., Martins, H. and Döscher, R. (2020) Warmer climate projections in EC-Earth3-veg: the role of changes in the greenhouse gas concentrations from CMIP5 to CMIP6. *Environmental Research Letters*, 15(5), 054020.

Xie, Y., Wang, X. and Silander, J.A. (2015) Deciduous forest responses to temperature, precipitation, and drought imply complex climate change impacts. *Proceedings of the National Academy of Sciences*, 112(44), 13585–13590.

Xu, C., McDowell, N.G., Fisher, R.A., Wei, L., Sevanto, S., Christoffersen, B.O., Weng, E. and Middleton, R.S. (2019b) Increasing impacts of extreme droughts on vegetation productivity under climate change. *Nature Climate Change*, 9(12), 948–953.

Xu, L., Chen, N. and Zhang, X. (2019a) Global drought trends under 1.5 and 2° C warming. *International Journal of Climatology*, 39(4), 2375–2385.

Yevjevich, V.M. (1967) Objective approach to definitions and investigations of continental hydrologic droughts, An. *Hydrology Papers (Colorado State University); no. 23.*

Zampieri, M., Ceglar, A., Dentener, F. and Toreti, A. (2017) Wheat yield loss attributable to heat waves, drought and water excess at the global, national and subnational scales. *Environmental Research Letters*, 12(6), 064008.

Zargar, A., Sadiq, R., Naser, B. and Khan, F.I. (2011) A review of drought indices. *Environmental Reviews*, 19, 333–349.

Zhang, D., Wang, G. and Zhou, H. (2011) Assessment on agricultural drought risk based on variable fuzzy sets model. *Chinese Geographical Science*, 21(2), 167–175.

Zhang, L., Xiao, J., Li, J., Wang, K., Lei, L. and Guo, H. (2012) The 2010 spring drought reduced primary productivity in southwestern China. *Environmental Research Letters*, 7(4), 045706.

Zhao, C., Liu, B., Piao, S., Wang, X., Lobell, D.B., Huang, Y., Huang, M., Yao, Y., Bassu, S., Ciais, P., Durand, J.-L., Elliott, J., Ewert, F., Janssens, I.A., Li, T., Lin, E., Liu, Q., Martre, P., Müller, C., Peng, S., Peñuelas, J., Ruane, A.C., Wallach, D., Wang, T., Wu, D., Liu, Z., Zhu, Y., Zhu, Z. and Asseng, S. (2017) Temperature increase reduces global yields of major crops in four independent estimates. *Proceedings of the National Academy of Sciences*, 114(35), 9326–9331.

Zhao, T. and Dai, A. (2015) The magnitude and causes of global drought changes in the twenty-first century under a low–moderate emissions scenario. *Journal of Climate*, 28(11), 4490–4512.

Zhao, T. and Dai, A. (2017) Uncertainties in historical changes and future projections of drought. Part II: model-simulated historical and future drought changes. *Climatic Change*, 144(3), 535–548.

Zittis, G., Hadjinicolaou, P., Klangidou, M., Proestos, Y. and Lelieveld, J. (2019) A multi-model, multi-scenario, and multi-domain analysis of regional climate projections for the Mediterranean. *Regional Environmental Change*, 19, 2621–2635.

Zscheischler, J., Westra, S., van den Hurk, B.J.J.M., Seneviratne, S. I., Ward, P.J., Pitman, A., AghaKouchak, A., Bresch, D.N., Leonard, M., Wahl, T. and Zhang, X. (2018) Future climate risk from compound events. *Nature Climate Change*, 8, 469–477. https://doi.org/10.1038/s41558-018-0156.

SUPPORTING INFORMATION

Additional supporting information may be found online in the Supporting Information section at the end of this article.

How to cite this article: Spinoni, J., Barbosa, P., Bucchignani, E., Cassano, J., Cavazos, T., Cescatti, A., Christensen, J. H., Christensen, O. B., Coppola, E., Evans, J., Forzieri, G., Geyer, B., Giorgi, F., Jacob, D., Katzfey, J., Koenigk, T., Laprise, R., Lennard, C. J., Levent Kurnaz, M., ... Dosio, A. (2021). Global exposure of population and land-use to meteorological droughts under different Warming Levels and Shared Socioeconomic Pathways: A Coordinated Regional Climate Downscaling Experiment-based study. *International Journal of Climatology*, 1–28. https://doi.org/10.1002/joc.7302